Electronic Supplementary Information

Crystal-to-crystal transformations and photoluminescence changes in the Cu(I) coordination networks based on a formamidinate ligand

Wayne Hsu,[a] Kuan-Ting Chen,[a] Yu-Sian Li,[a] Po-Wen Cheng,[a]
Tsun-Ren Chen[b] and Jhy-Der Chen[a]*

[a]*Department of Chemistry, Chung-Yuan Christian University, Chung-Li, Taiwan, R.O.C.*

[b]*Department of Applied Chemistry, National Pingtung University, Ping-Tung, Taiwan, R.O.C.*

Table S1. Crystallographic Data for **2d** and **2e**.

	2d	**2e**
formula	$C_{22}H_{18}Cu_2N_8$	$C_{44}H_{36}Cu_4N_{16}$
fw	521.52	1043.05
temperature/K	100(2)	100(2)
space group	*I*-4	*I*-4*c*2
a, Å	14.8613(19)	14.9835(3)
b, Å	14.8613(19)	14.9835(3)
c, Å	38.880(5)	37.582(2)
β, deg	90	90
V, Å^3	8586.9(19)	8437.3(6)
Z	8	8
D_{calc}, g/cm^3	0.807	1.642
μ, mm^{-1}	1.004	2.044
$2\theta_{max}$, deg	56.80	56.66
no. of reflns meased	36989	36261
no. of reflns used (R_{int})	10655, 0.1977	5245, 0.1734
data completeness (%)	99.1	99.6
no. of params	132	290
GOF on F^2	1.453	1.102
R_1[a]	0.1468	0.0972
wR_2[b], final *R* [$I>2\sigma(I)$]	0.3405	0.2461
R_1[a]	0.2002	0.1887
wR_2[b] (all data)	0.3555	0.2913

[a]$R_1 = \Sigma||F_o| - |F_c|| / \Sigma|F_o|$. [b]$wR_2 = [\Sigma w(F_o^2 - F_c^2)^2 / \Sigma w(F_o^2)^2]^{1/2}$. $w = 1 / [\sigma^2(F_o^2) + (ap)^2 + (bp)]$, $p = [\max(F_o^2 \text{ or } 0) + 2(F_c^2)] / 3$. a = 0.1998, b = 47.6514, **2d**; a = 0.1001, b = 167.2205, **2e**.

Table S2. Selected bond lengths (Å) and cavity volume (Å^3) for **1a** – **1c**.

	1a	**1b**	**1c**
Cu···Cu(A)	2.5444(5)	2.5470(5)	2.5348(3)
Cu-N(2)	1.9441(16)	1.9481(17)	1.9408(12)
Cu-N(3A)	1.9484(17)	1.9557(16)	1.9439(12)
Cu-N(4B)	2.1189(17)	2.1310(17)	2.1131(13)
Inter- π···π	3.90	4.48	3.97
cavity volume	801.42	791.33	774.81
C(4)-H---O	2.443(5)	2.433(5)	2.663(2)
C(8)-H---O		2.347(5)	

Symmetry transformations used to generate equivalent atoms:
(A): -x + 1, -y + 1, -z + 1; (B): -x + 1, y + 1/2, -z + 3/2 for **1a** and **1c**. (A): -x + 1, -y, -z; (B): x, -y + 1/2, z – 1/2 for **1b**.

Table S3. Selected bond lengths (Å) for **2a** - **2c**.

	2a	**2b**	**2c**
Cu(1) ···Cu(2)	2.5099(7)	2.5027(5)	2.5035(9)
Cu(3) ···Cu(3A)	2.5283(9)	2.5317(7)	2.5463(12)
Cu(4) ···Cu(4A)	2.5027(8)	2.5067(6)	2.4968(13)
Cu(1)-N(13)	2.130(3)	2.143(2)	2.157(4)
Cu(2)-N(9)	2.191(4)	2.157(3)	2.129(5)
Cu(3)-N(5B)	2.082(4)	2.076(2)	2.075(4)
Cu(4)-N(4C)	2.142(3)	2.152(2)	2.155(4)
Cu(1)-N(2)	1.969(3)	1.965(2)	1.967(4)
Cu(1)-N(6)	1.972(3)	1.978(2)	1.981(4)
Cu(2)-N(3)	1.933(3)	1.929(2)	1.933(4)
Cu(2)-N(7)	1.927(3)	1.928(2)	1.935(4)
Cu(3)-N(11)	1.954(3)	1.944(2)	1.943(4)
Cu(3)-N(10A)	1.955(3)	1.961(2)	1.964(4)
Cu(4)-N(14)	1.948(3)	1.949(2)	1.951(4)
Cu(4)-N(15A)	1.952(3)	1.950(2)	1.949(4)
intra- π···π	3.51, 3.75, 3.76	3.49, 3.73, 3.74	3.51, 3.72, 3.74
O(1')-H---N(16)	1.969(6)	1.872(5)	
O(2')-H---N(12)	2.105(7)		
C(38)-H---O(1)		2.551(3)	
C(26)-H---O(1)			2.496(7)

Symmetry transformations used to generate equivalent atoms:
(A): -x + 1, y, -z + 3/2; (B): x + 1/2, y - 1/2, z;
(C): -x + 1/2, y + 1/2, -z + 3/2

Table S4. Selected bond lengths (Å) for **3a** and **3b**.

	3a	**3b**
Cu(1) ···Cu(2)	2.5540(9)	2.5716(4)
Cu(1)-N(4A)	2.153(5)	2.114(2)
Cu(1)-N(5B)	2.107(5)	2.174(2)
Cu(3)-N(1)	1.899(9)	1.876(2)
Cu(3)-N(8C)	1.873(8)	1.888(3)
Cu(3')-N(1)	1.893(16)	
Cu(3')-N(8C)	1.938(16)	
Cu(1)-N(2)	1.960(5)	1.935(2)
Cu(1)-N(6)	1.965(5)	1.930(2)
Cu(2)-N(3)	1.927(5)	1.968(2)
Cu(2)-N(7)	1.932(5)	1.973(2)
intra- π···π	4.00	3.98
C(22)-H---F(1)	2.922(11)	
C(22)-H---F(2)	2.614(11)	
C(22)-H---F(4)	2.566(14)	
C(18)-H---O(2')	2.640(2)	
O(1)---Cu(3)		2.861(6)
C(22C)-H---O(1)		2.580(8)
C(1)-H---O(1)		2.823(6)

Symmetry transformations used to generate equivalent atoms: (A): x, -y + 1/2, z + 1/2; (B): -x + 1, y – 1/2, -z + 1/2; (C) x – 1, y, z, for **3a**. (A): -x + 1, y - 1/2, -z + 1/2; (B): x, y + 1/2, z – 1/2; (C): x - 1, y, z, for **3b**.

Table S5. Thermal gravimetric analyses of complexes **1a** - **2b**.

Complex	Weight loss of solvent, T, ^{o}C (calc/found), %	Weight loss of 4-pyf^{-}, T, ^{o}C (calc/found), %
1a	80-170 (18.2/19.8)	280-750 (61.8/60.6)
1b	85-180 (21.9/19.7)	285-800 (59.1/60.4)
1c	80-165 (21.7/20.2)	280-700 (59.2/59.4)
2a	110-195 (5.8/6.8)	290-760 (71.3/71.6)
2b	60-200 (8.1/8.6)	295-755 (69.5/68.3)

Table S6. DSC parameters of complexes **1a** - **3b**.

complex	T_g, ^oC	*anti* → *syn* $T_c/^oC$, $\Delta H/J \cdot g^{-1}$	solvent loss $T_m/^oC$, $\Delta H/J \cdot g^{-1}$	phase change $T_c/^oC$, $\Delta H/J \cdot g^{-1}$
1a	55	81, -1.54	153, 9.13	201, -1.60
1b	52	73, -0.65	179, 12.07	199, -1.08
1c	54	81, -0.22	155, 2.48	196, -0.35
2a			86, 0.25	202, -0.25
			172, 2.18	
2b			75, 0.40	203, -0.33
			143, 1.92	
3a			105, 21.08	
3b			135, 26.38	

Table S7. Solid-state luminescence data for crystalline samples of **2a** - **3b** at room temperature.

Complex	Emission	
	λ_{em}, nm	λ_{ex}, nm
2a	587	480
2b	588	485
3a	597	496
3b	590	481

Table S8. The contributions of d orbitals to each molecular orbitals of *syn*- and *anti*- geometrical complexes (%)

	HOMO-2	HOMO-1	HOMO	LUMO	LUMO+1	LUMO+2
Anti-	$^{87}a_u$	$^{88}a_u$	$^{87}a_g$	$^{88}a_g$	$^{89}a_u$	$^{90}a_u$
d_{z^2}	19.28	37.62	24.56	0.84	1.43	2.30
d_{xz}	14.79	10.73	8.72	0.54	0.10	1.04
d_{yz}	20.38	14.20	6.59	0.08	0.04	0.84
$d_{x^2-y^2}$	1.90	1.17	10.01	1.25	2.78	0.72
d_{xy}	6.29	3.54	13.38	0.48	1.81	1.75
Syn-	^{86}a	^{87}a	^{87}b	^{88}a	^{88}b	^{89}b
d_{z^2}	15.43	15.58	21.09	0.84	0.72	0.67
d_{xz}	12.55	16.45	4.53	1.01	0.46	0.23
d_{yz}	7.83	20.20	4.79	1.36	0.73	0.95
$d_{x^2-y^2}$	1.70	1.03	0.79	0.28	0.36	0.26
d_{xy}	13.89	7.99	29.85	0.44	0.73	0.44

Table S9. Adsorption of $CdCl_2$ by **1a** (0.32 g, 1 mmol)

$CdCl_2$ used (g/mmol)	$CdCl_2$ adsorbrd (g/mmol)	Cd/Cu ratio based on EDS	Formula based on EDS	EA calcd based on EDS. (%)	EA found (%)
0.092/0.50	0.069/0.38	0.34	$C_{14}H_{15}CuN_4O(CdCl_2)_{0.34}$	C, 44.11; H, 3.97; N, 14.70	C,43.07; H, 3.62; N, 14.37
0.18/1.00	0.11/0.60	0.62	$C_{14}H_{15}CuN_4O(CdCl_2)_{0.62}$	C, 38.88; H, 3.50; N, 12.95	C, 37.74; H, 3.72; N, 12.25
0.27/1.50	0.11/0.61	0.58	$C_{14}H_{15}CuN_4O(CdCl_2)_{0.58}$	C, 39.55; H, 3.56; N, 13.18	C, 39.27; H, 3.17; N, 13.13
0.37/2.00	0.10/0.57	0.59	$C_{14}H_{15}CuN_4O(CdCl_2)_{0.59}$	C, 39.38; H, 3.54; N, 13.12	C, 39.43; H, 3.68; N, 13.16

Table S10. Adsorption of $CdCl_2$ by **2a** (0.28 g, 1 mmol)

$CdCl_2$ used (g/mmol)	$CdCl_2$ adsorbrd (g/mmol)	Cd/Cu ratio based on EDS	Formula based on EDS	EA calcd based on EDS. (%)	EA found (%)
0.092/0.50	0.065/0.36	0.39	$C_{11.5}H_{11}CuN_4O_{0.5}(CdCl_2)_{0.39}$	C, 39.66; H, 3.18; N, 16.09	C, 40.19; H, 3.18; N, 16.16
0.18/1.00	0.11/0.61	0.66	$C_{11.5}H_{11}CuN_4O_{0.5}(CdCl_2)_{0.66}$	C, 34.72; H, 2.79; N, 14.09	C, 34.89; H, 2.86; N, 14.11
0.27/1.50	0.12/0.66	0.68	$C_{11.5}H_{11}CuN_4O_{0.5}(CdCl_2)_{0.68}$	C, 34.41; H, 2.76; N, 13.96	C, 34.25; H, 3.01; N, 14.04
0.37/2.00	0.13/0.71	0.67	$C_{11.5}H_{11}CuN_4O_{0.5}(CdCl_2)_{0.67}$	C, 34.56; H, 2.77; N, 14.02	C, 34.54; H, 2.86; N, 13.92

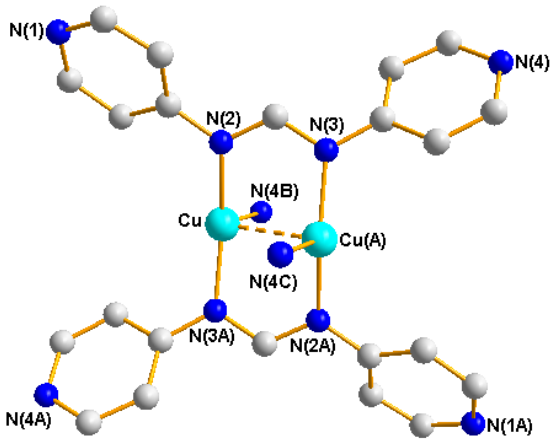

(a)

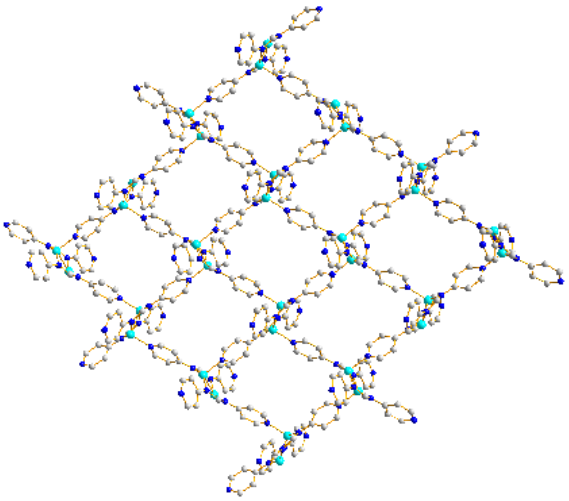

(b)

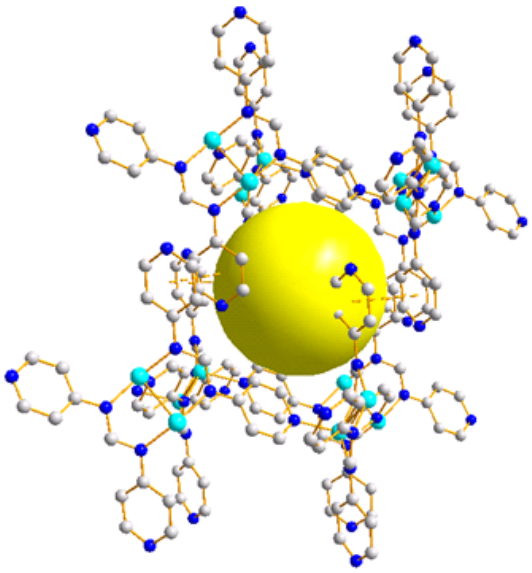

(c)

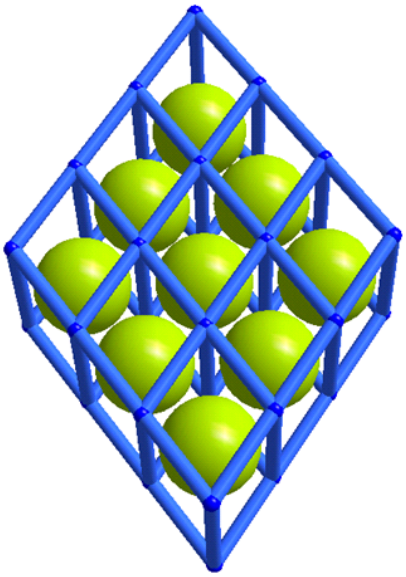

(d)

Fig. S1. (a) A representative drawing showing the coordination environment about the Cu(I) centers of **1a** - **1c**. Symmetry transformations used to generate equivalent atoms: (A) –x + 1,-y + 1, -z + 1; (B) –x + 1, y + 1/2, -z + 3/2; (C) –x + 1, y - 1/2, -z + 3/2 for **1a** and **1c**. (A) –x + 1, -y, -z; (B) x, -y + 1/2, z-1/2; (C) x, -y + 1/2, z + 1/2 for **1b**. (b) A representative drawing showing the 2D layer of **1a** – **1c**. (c) A drawing showing the supramolecular structure of **1a** – **1c** that is supported by the π-π stacking interactions. (d) A simplified schematic drawing showing the 3D supramolecular structure with cavities occupied by the solvents.

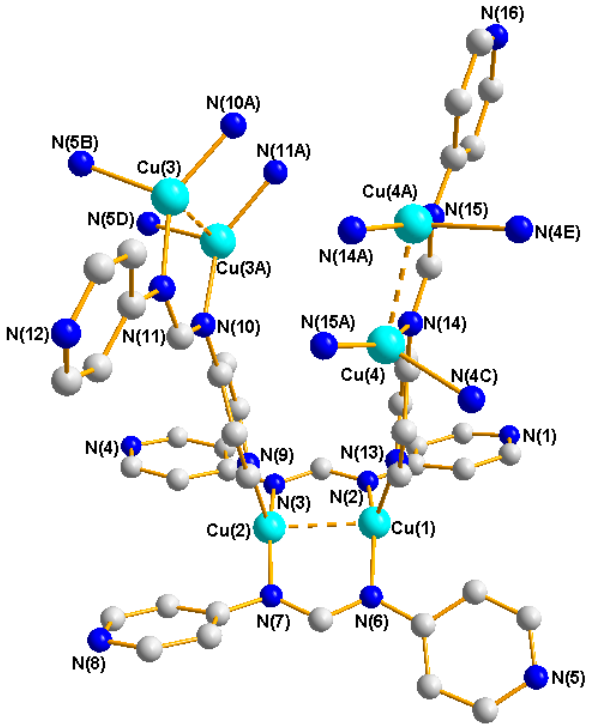
N(16)
N(10A)
N(5B)
Cu(3)
N(11A)
Cu(4A)
N(15)
N(5D)
N(4E)
N(14A)
Cu(3A)
N(12)
N(11)
N(10)
N(15A)
N(14)
Cu(4)
N(4C)
N(4)
N(9)
N(13)
N(1)
N(3)
N(2)
Cu(2)
Cu(1)
N(7)
N(6)
N(8)
N(5)

(a)

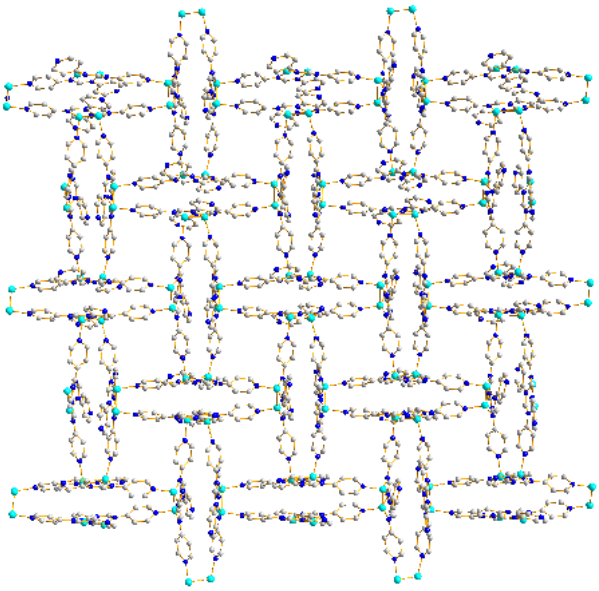

(b)

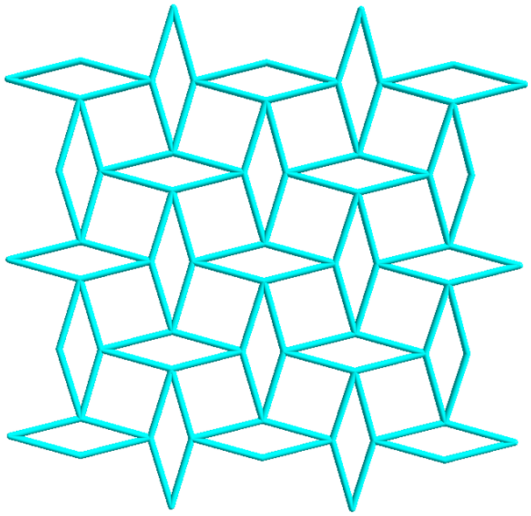

(c)

Fig. S2. (a) A representative drawing showing the coordination environment about the Cu(I) centers of **2a** and **2b**. Symmetry transformations used to generate equivalent atoms: (A) –x + 1, y, -z + 3/2; (B) x + 1/2, y - 1/2, z; (C) -x + 1/2, y + 1/2, -z + 3/2; (D) –x + 1/2, y - 1/2, -z + 3/2; (E) x - 1/2, y + 1/2, z. (b) A representative drawing showing the 2D layer of **2a** and **2b**. (c) A schematic drawing showing the orientations of the dangling pyridyl nitrogen atoms.

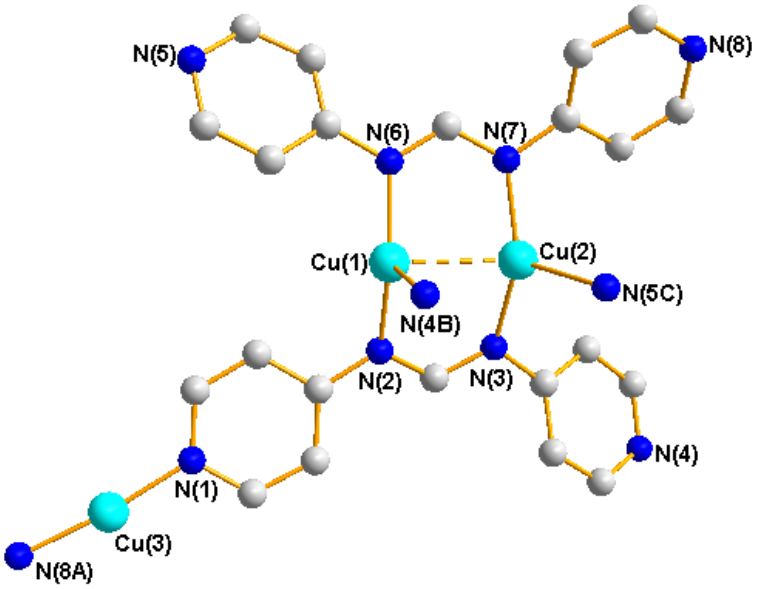

Fig. S3. A representative drawing showing the coordination environment about the Cu(I) centers of **3a** and **3b**. Symmetry transformations used to generate equivalent atoms: (A) x + 1, y, z; (B) –x + 1, y - 1/2, -z + 3/2; (C) x, -y + 1/2, z + 1/2.

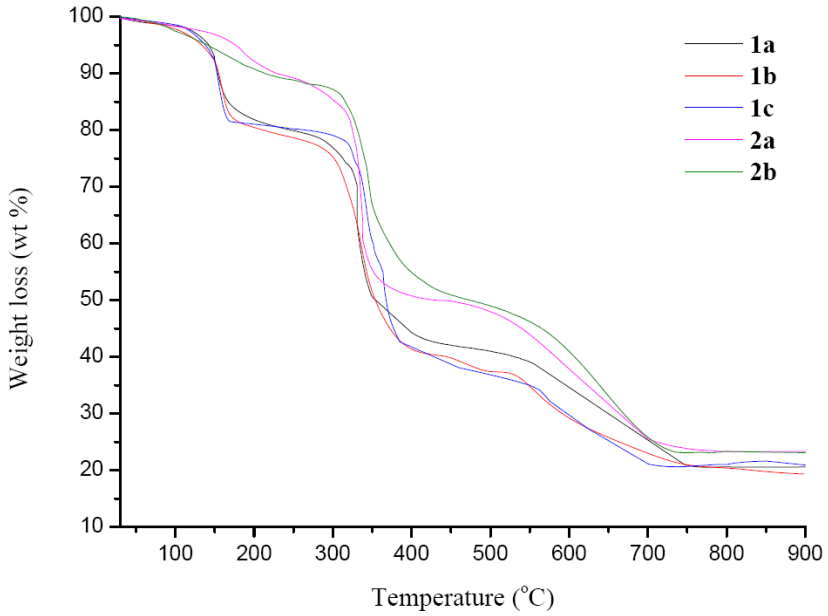
Weight loss (wt %)
Temperature (°C)
1a
1b
1c
2a
2b

(a)

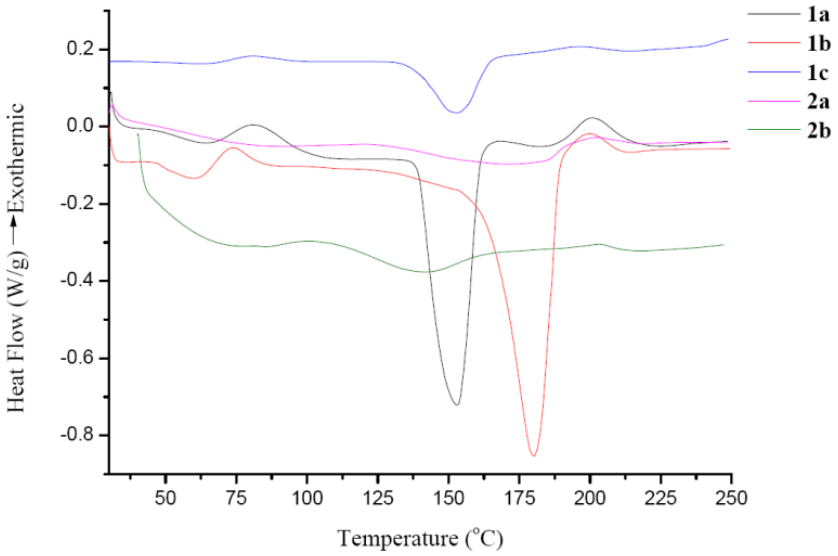
Heat Flow (W/g) →Exothermic
Temperature (°C)
1a
1b
1c
2a
2b

(b)

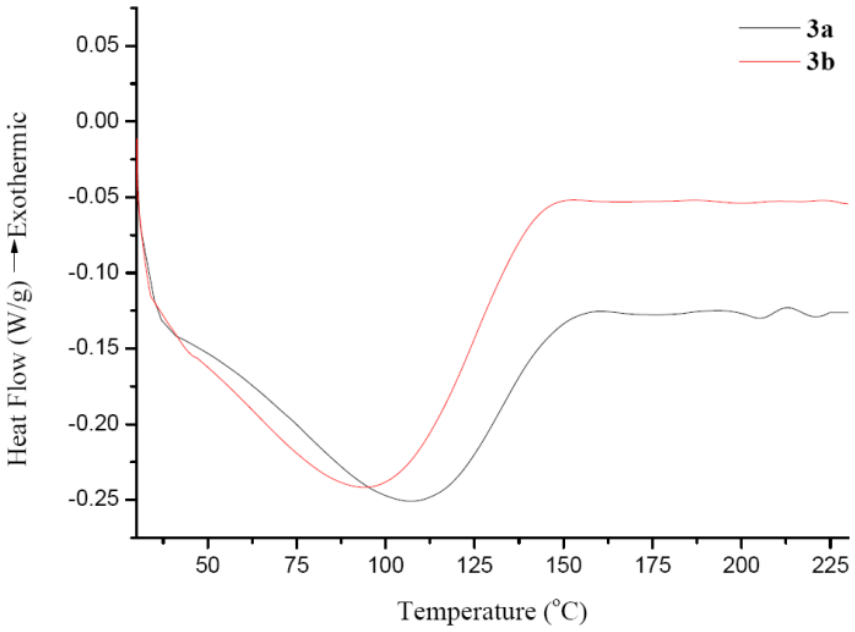

(c)

Fig. S4. (a) TGA curves for complexes **1a** - **2b**. (b) DSC curves of **1a** - **2b**. (c) DSC curves of **3a** and **3b**.

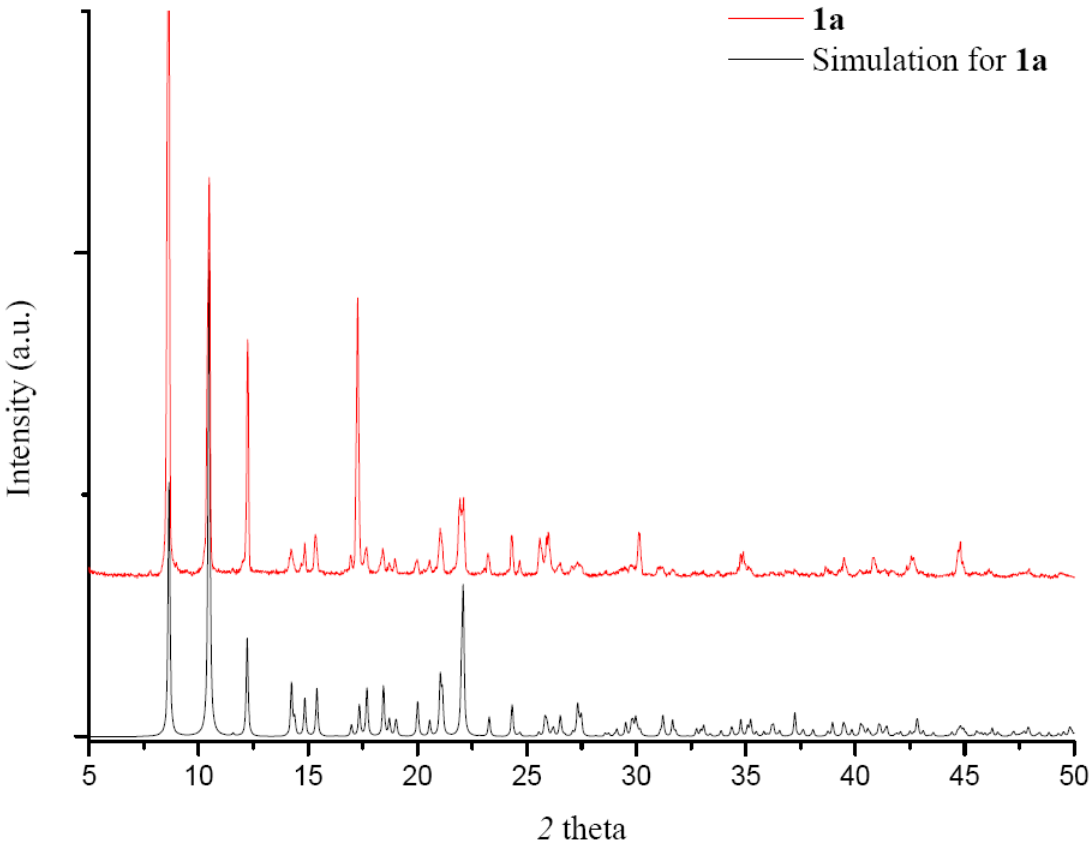

Fig. S5. Simulated and experimental powder XRD patterns for **1a**.

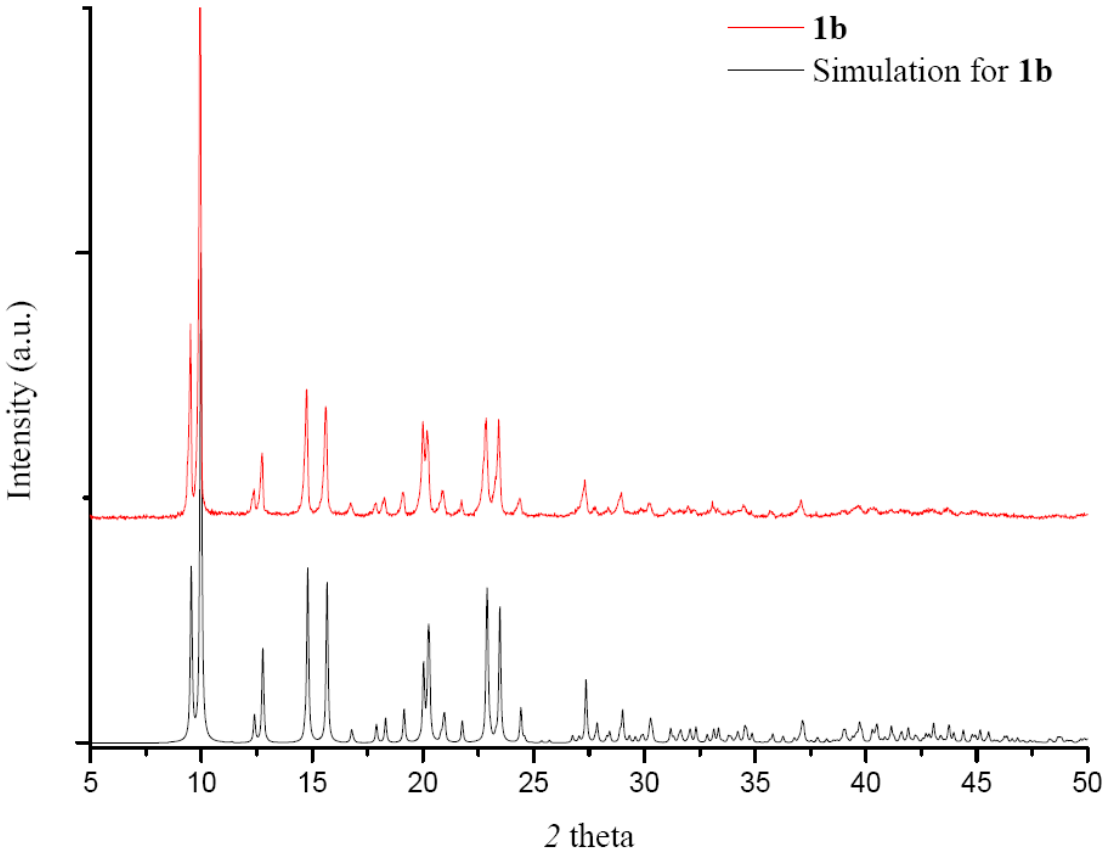

Fig. S6. Simulated and experimental powder XRD patterns for **1b**.

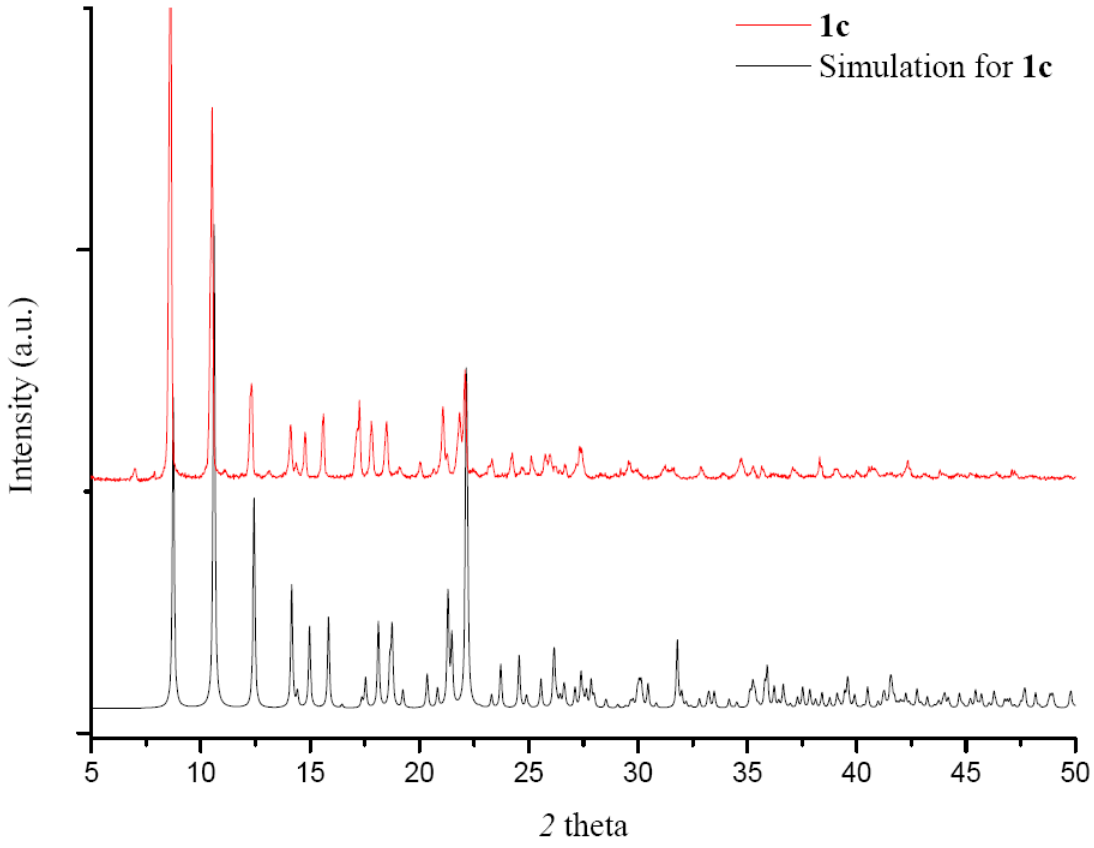

Fig. S7. Simulated and experimental powder XRD patterns for **1c**.

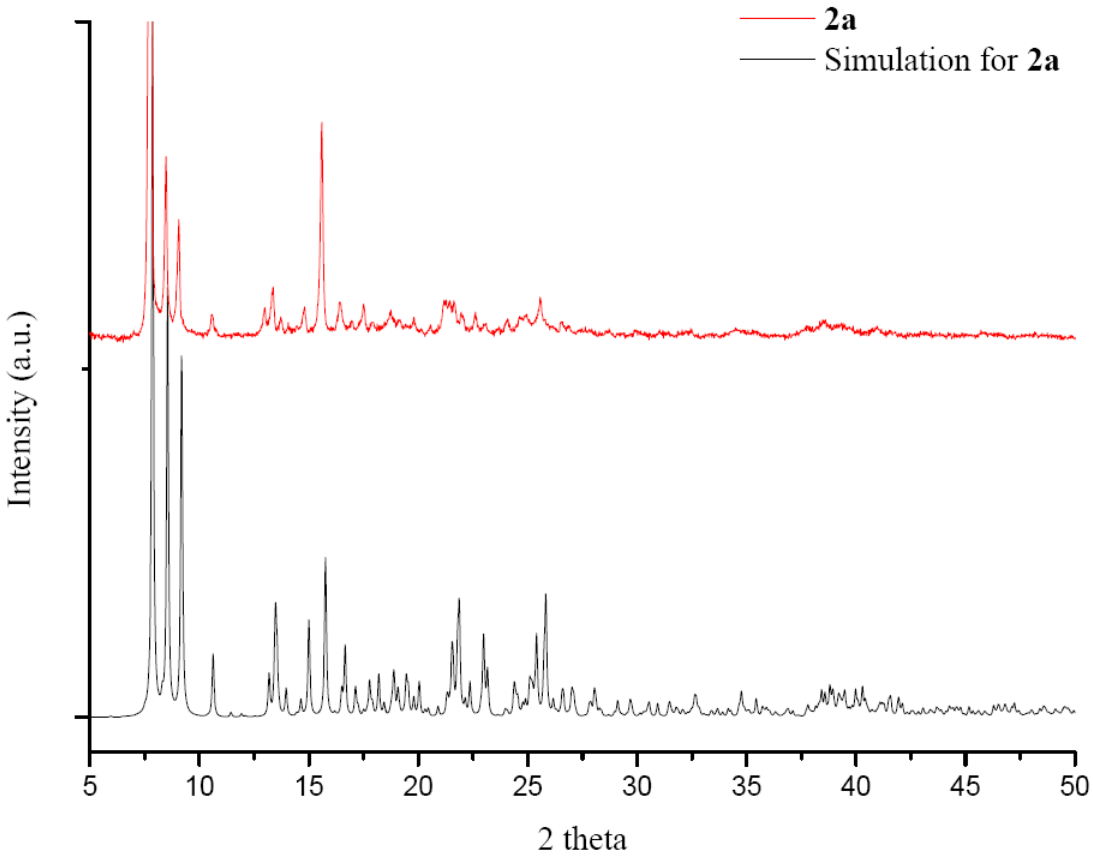

Fig. S8. Simulated and experimental powder XRD patterns for **2a**.

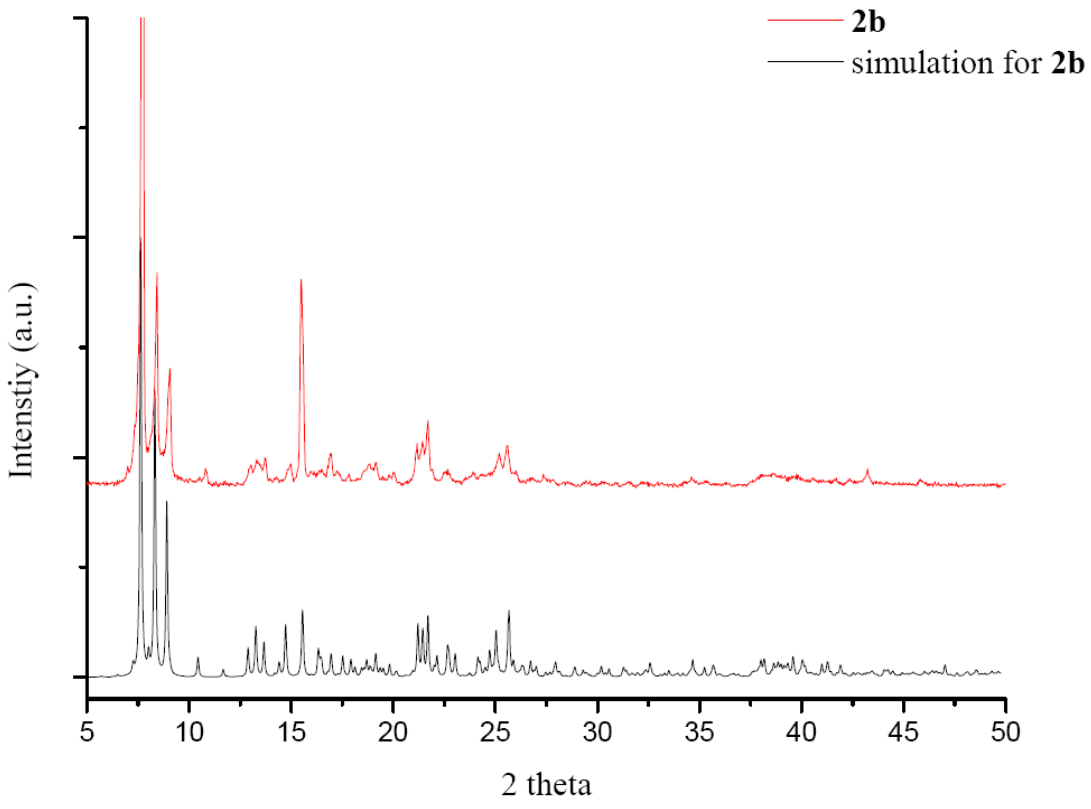

Fig. S9. Simulated and experimental powder XRD patterns for **2b**.

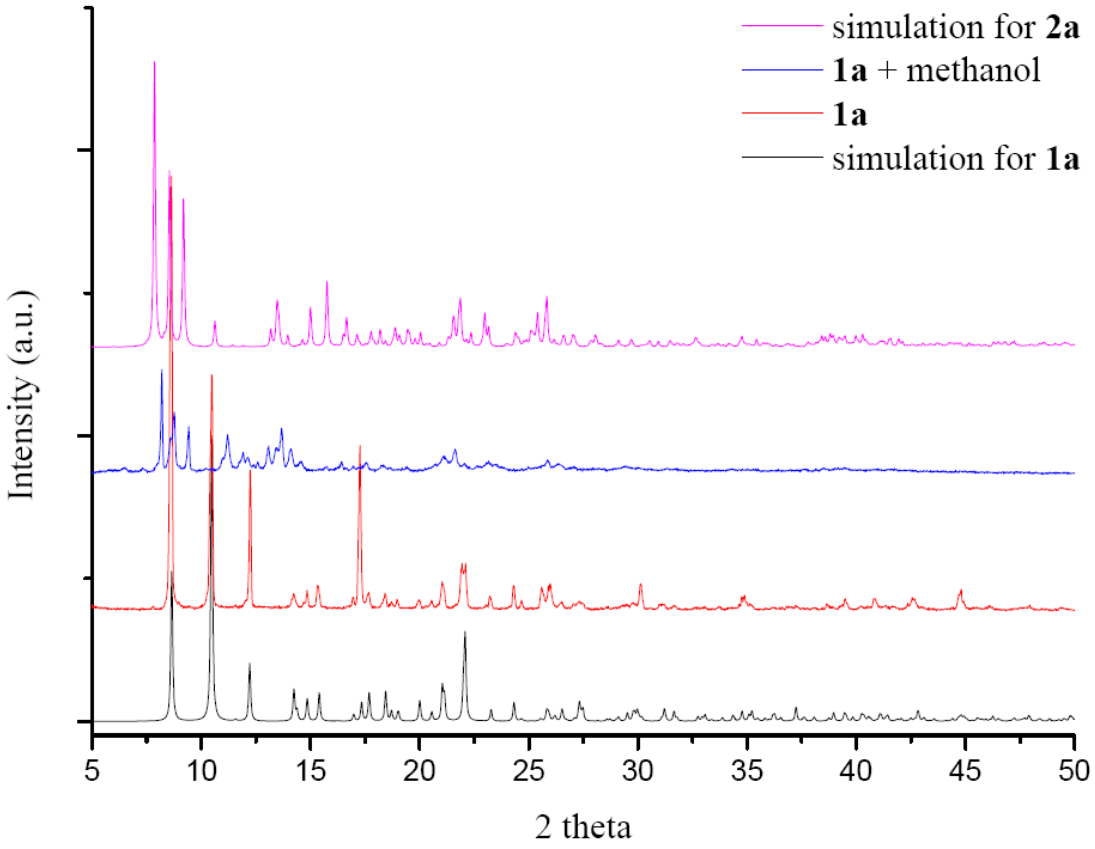

Fig. S10. The simulated and solvent-induced SCSC transformation PXRD patterns for **1a** to **2a**.

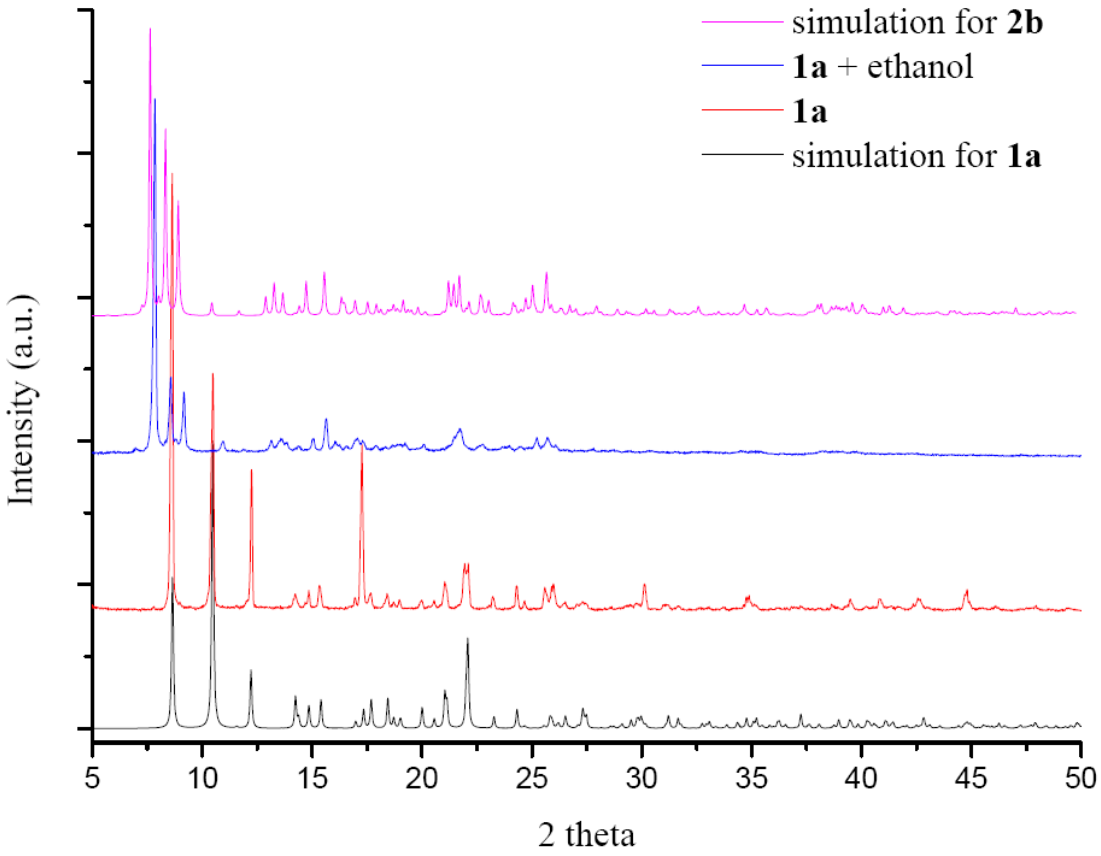

Fig. S11. The simulated and solvent-induced SCSC transformation PXRD patterns for **1a** to **2b**.

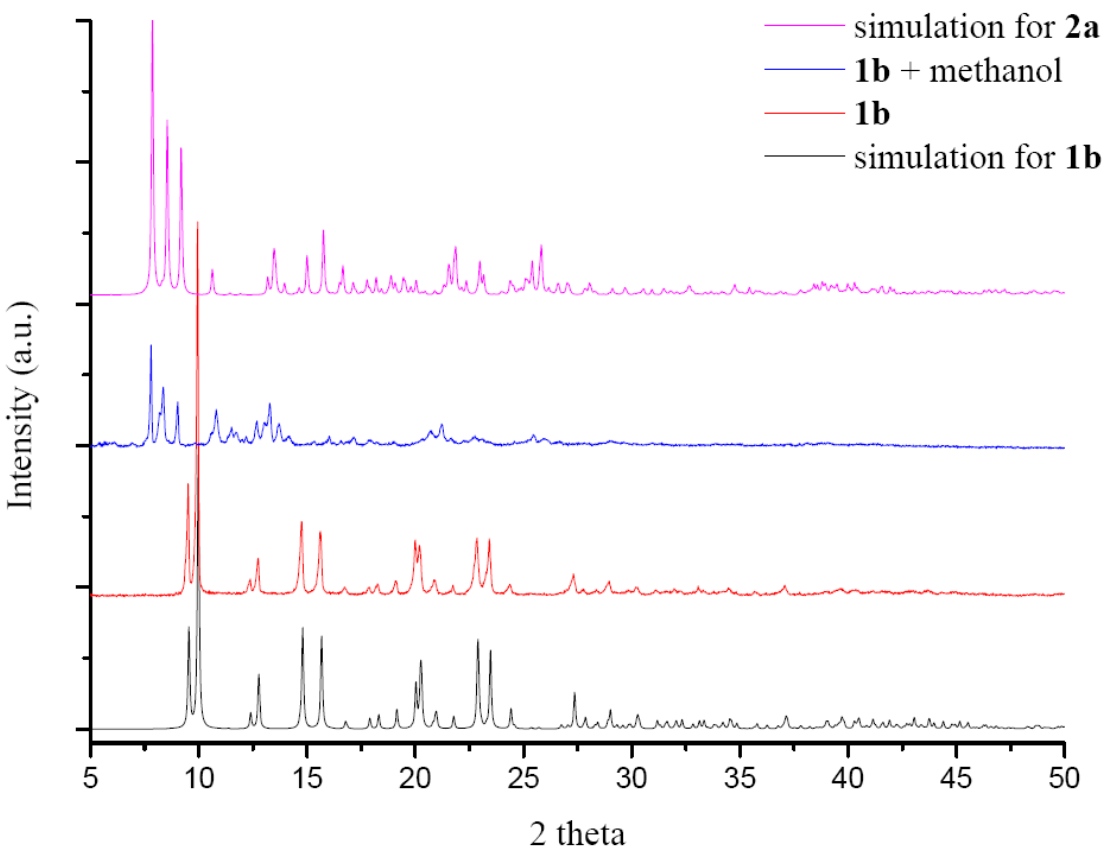

Fig. S12. The simulated and solvent-induced SCSC transformation PXRD patterns for **1b** to **2a**.

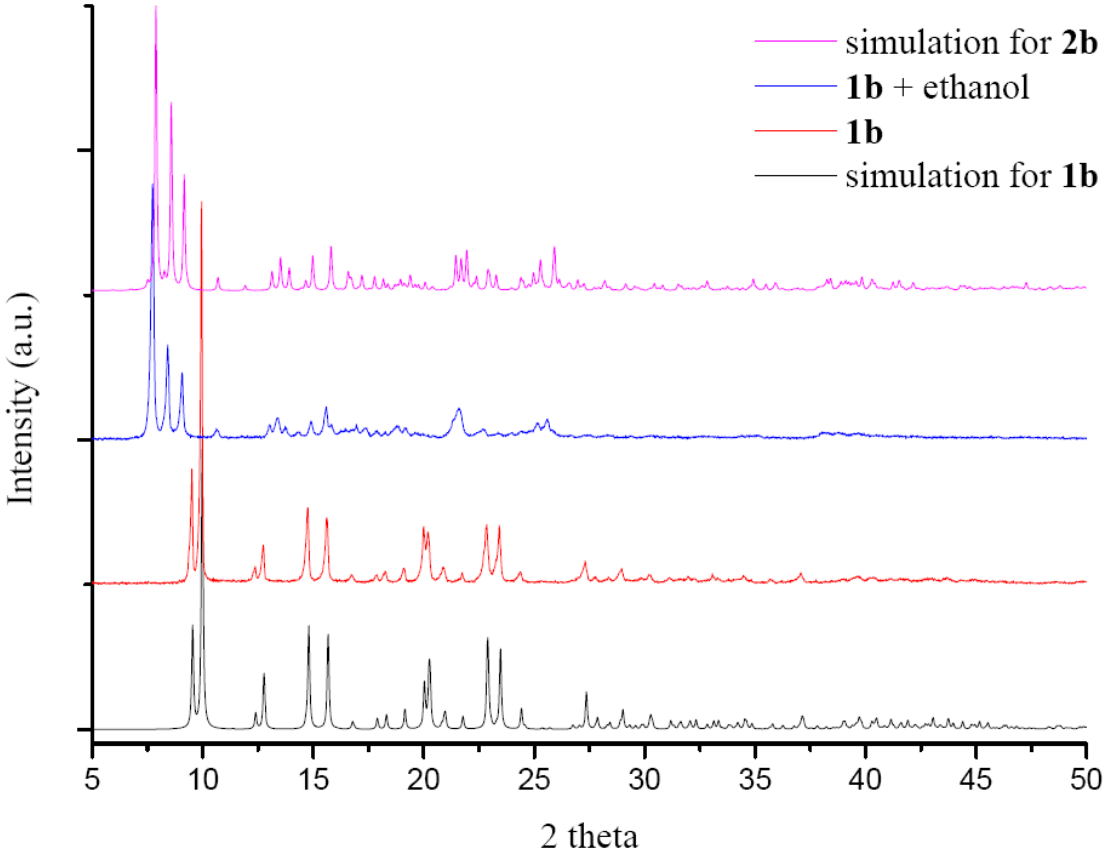

Fig. S13. The simulated and solvent-induced SCSC transformation PXRD patterns for **1b** to **2b**.

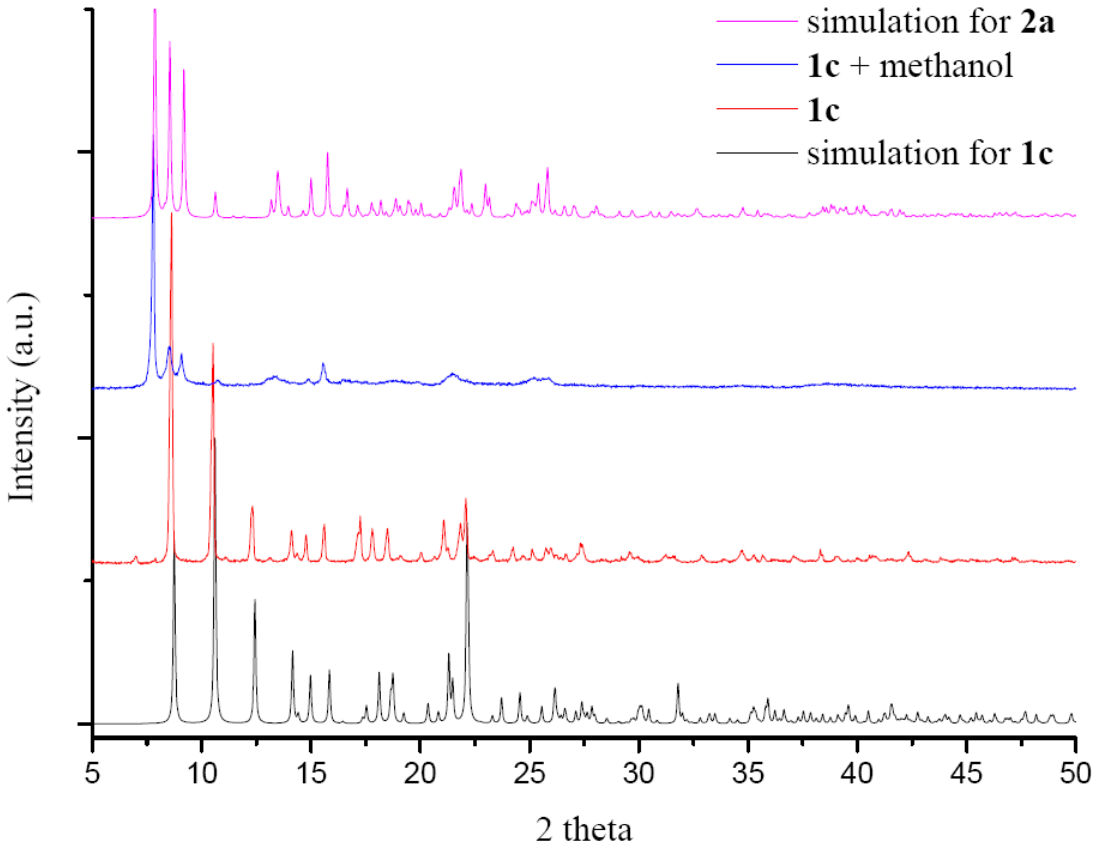

Fig. S14. The simulated and solvent-induced SCSC transformation PXRD patterns for **1c** to **2a**.

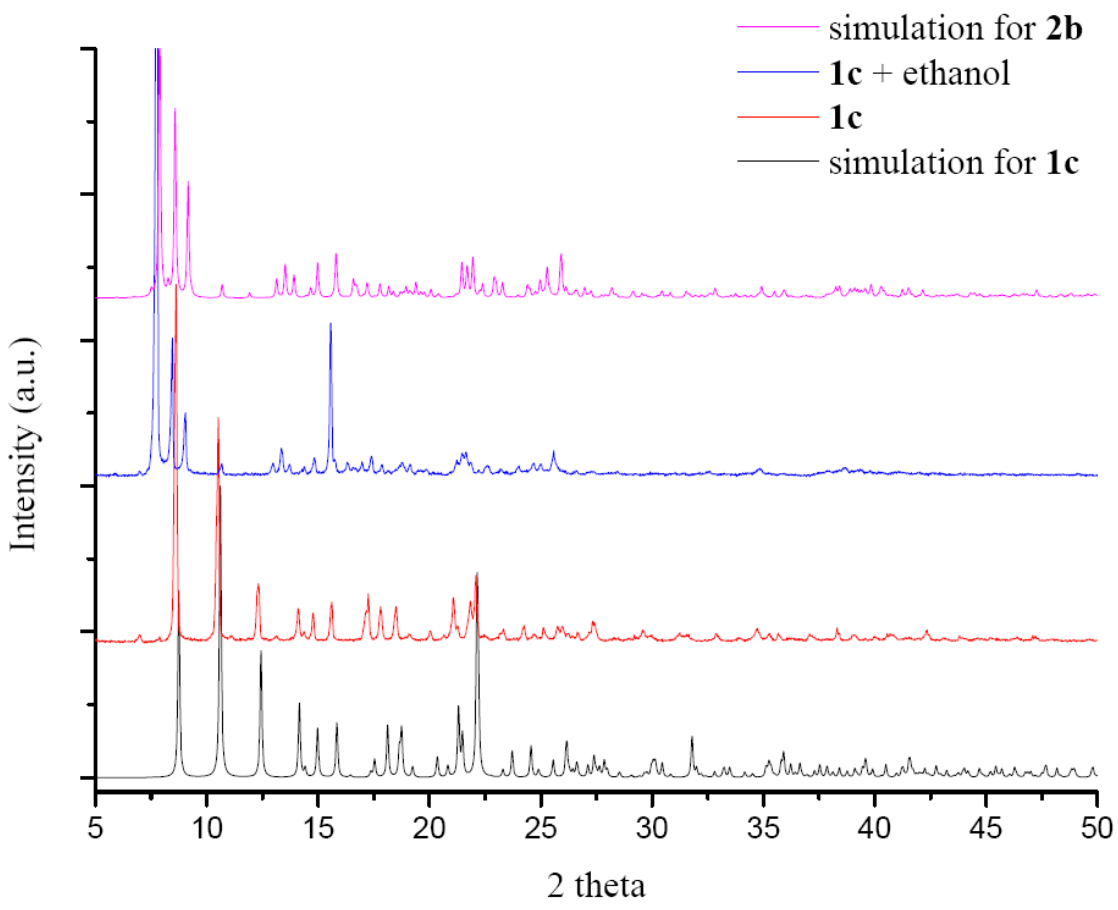

Fig. S15. The simulated and solvent-induced SCSC transformation PXRD patterns for **1c** to **2b**.

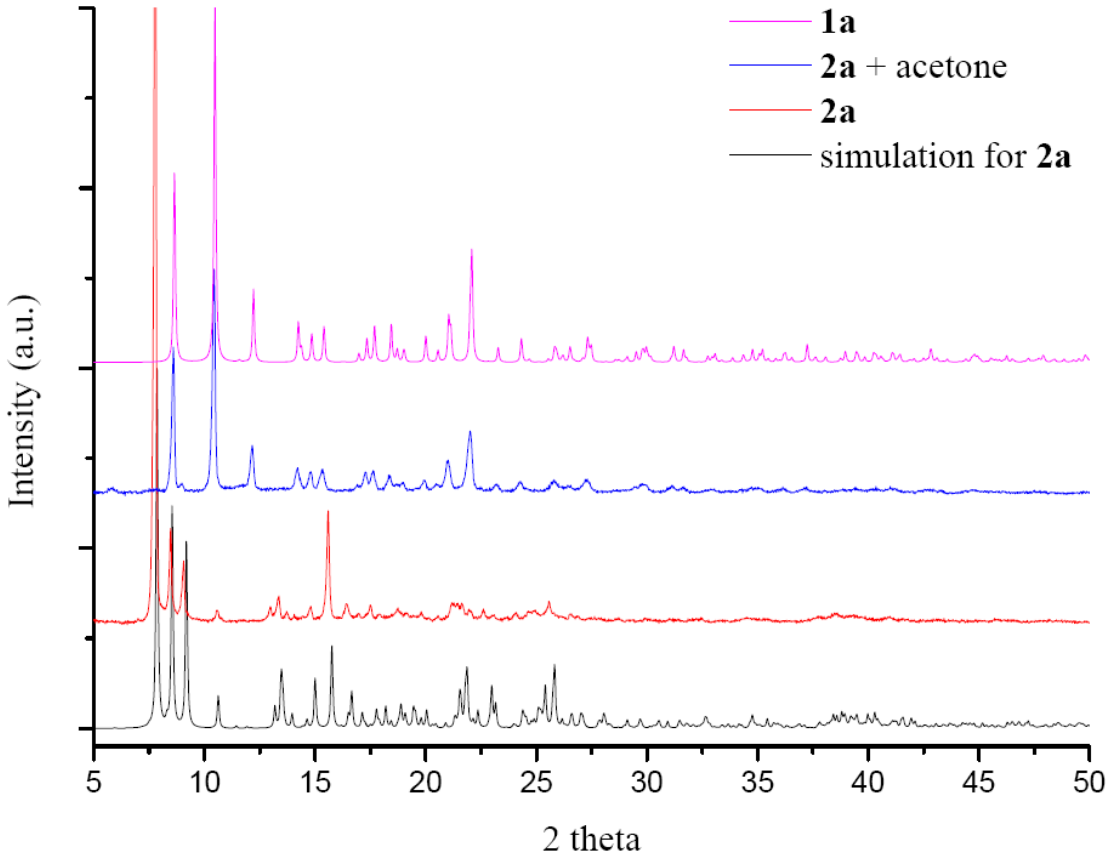

Fig. S16. The simulated and solvent-induced SCSC transformation PXRD patterns for **2a** to **1a**.

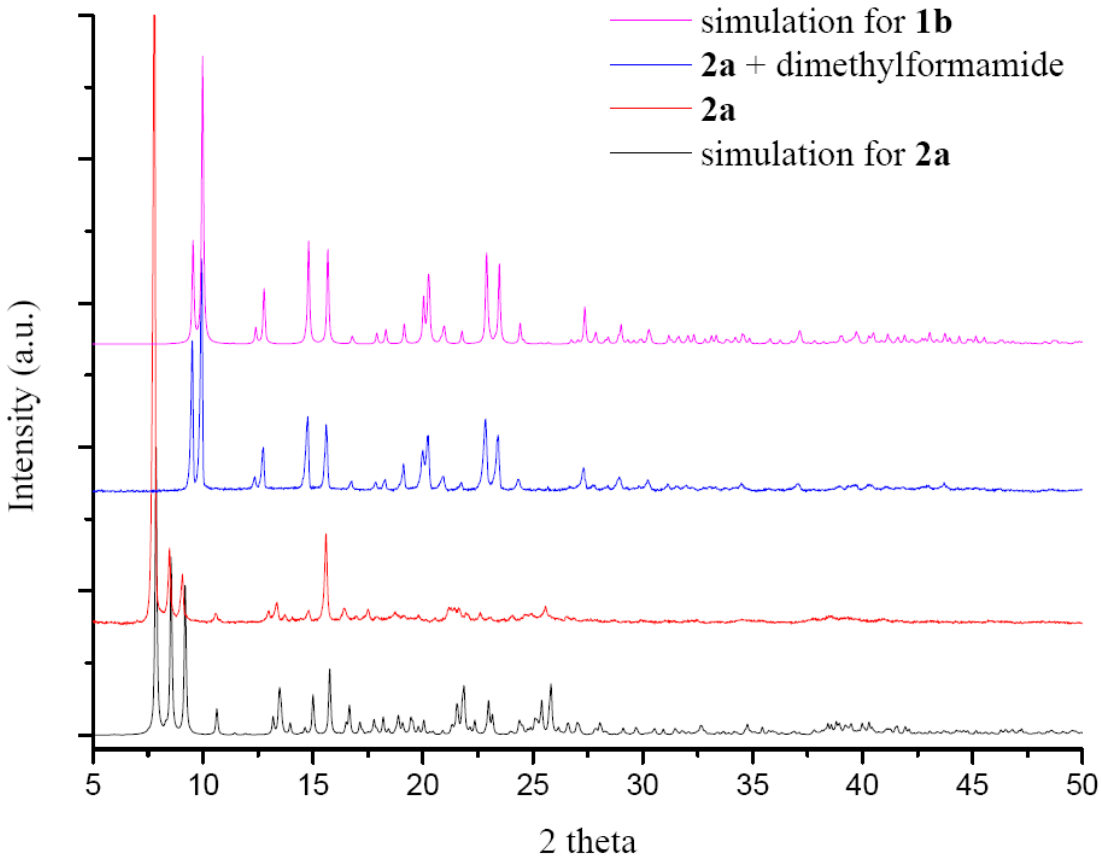

Fig. S17. The simulated and solvent-induced SCSC transformation PXRD patterns for **2a** to **1b**.

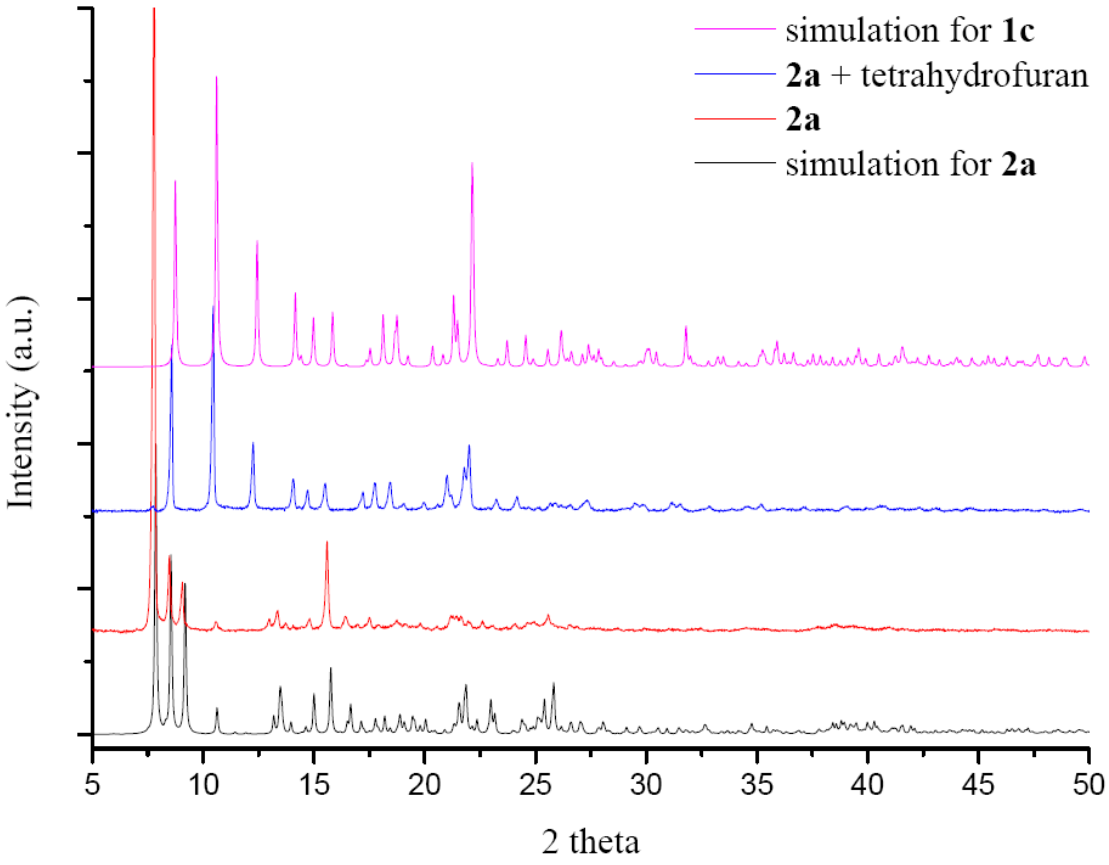

Fig. S18. The simulated and solvent-induced SCSC transformation PXRD patterns for **2a** to **1c**.

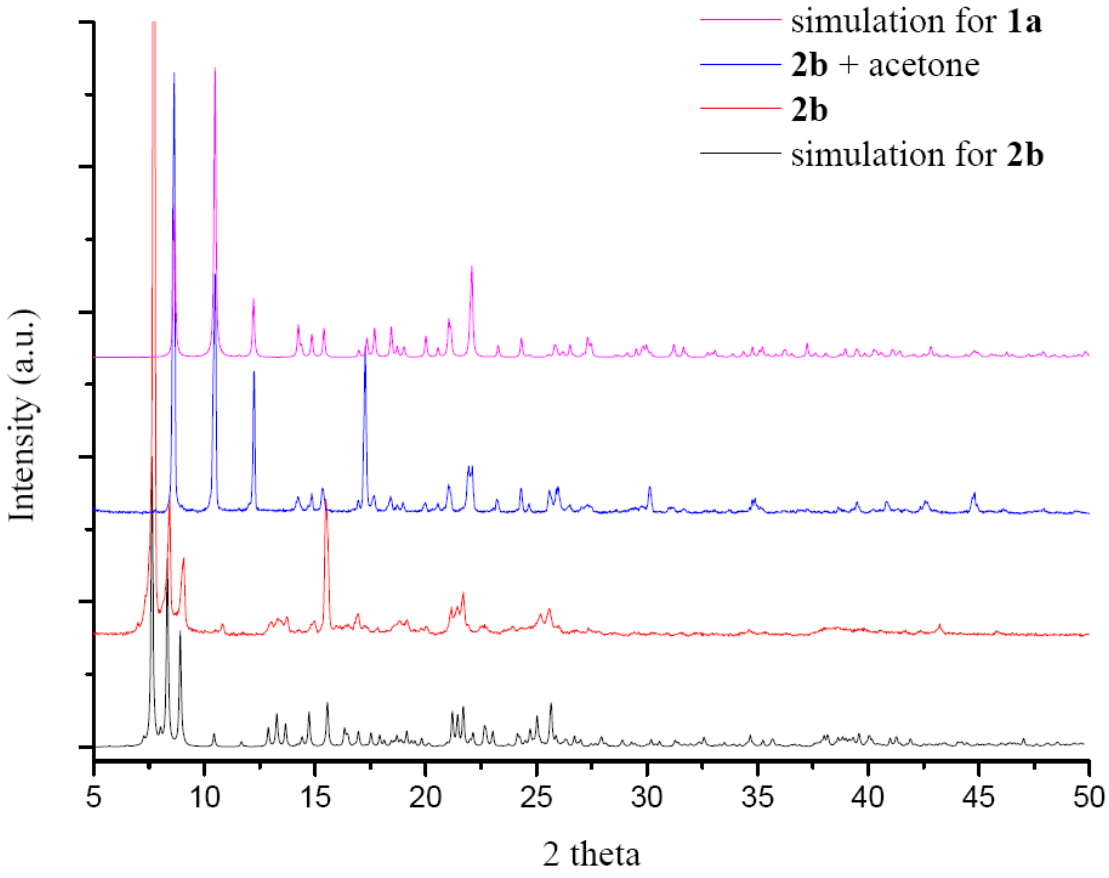

Fig. S19. The simulated and solvent-induced SCSC transformation PXRD patterns for **2b** to **1a**.

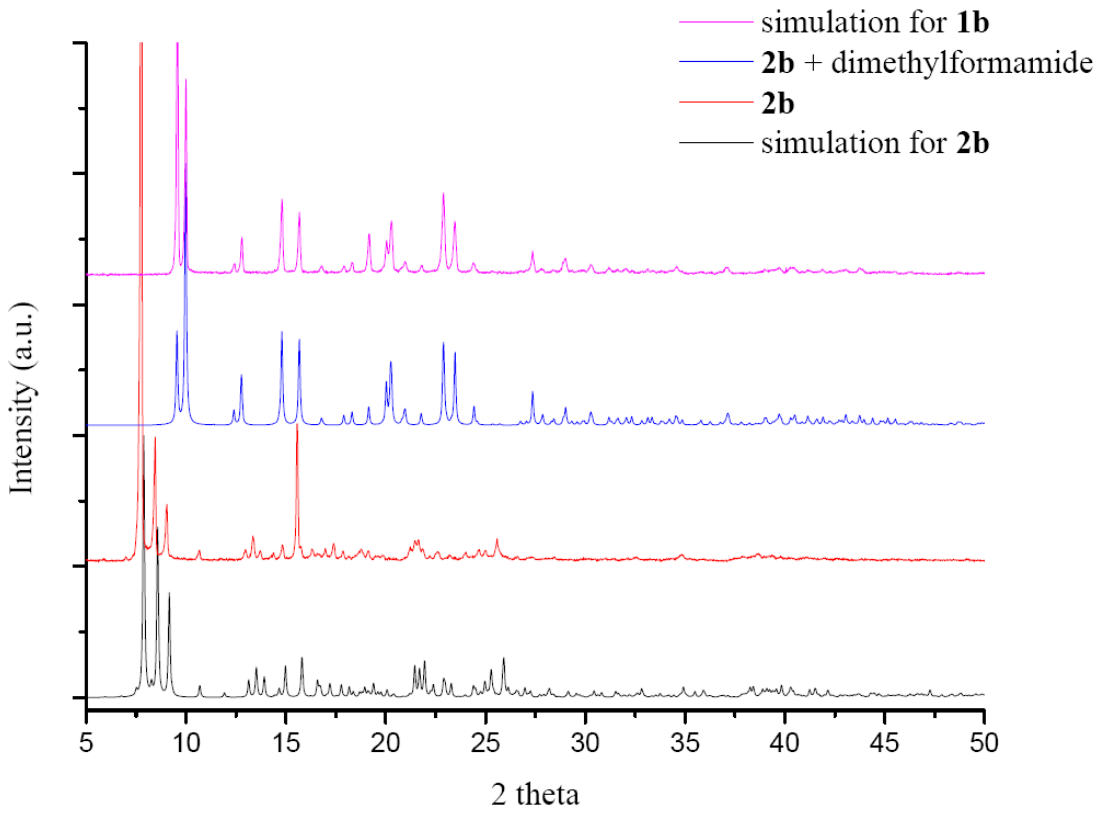

Fig. S20. The simulated and solvent-induced SCSC transformation PXRD patterns for **2b** to **1b**.

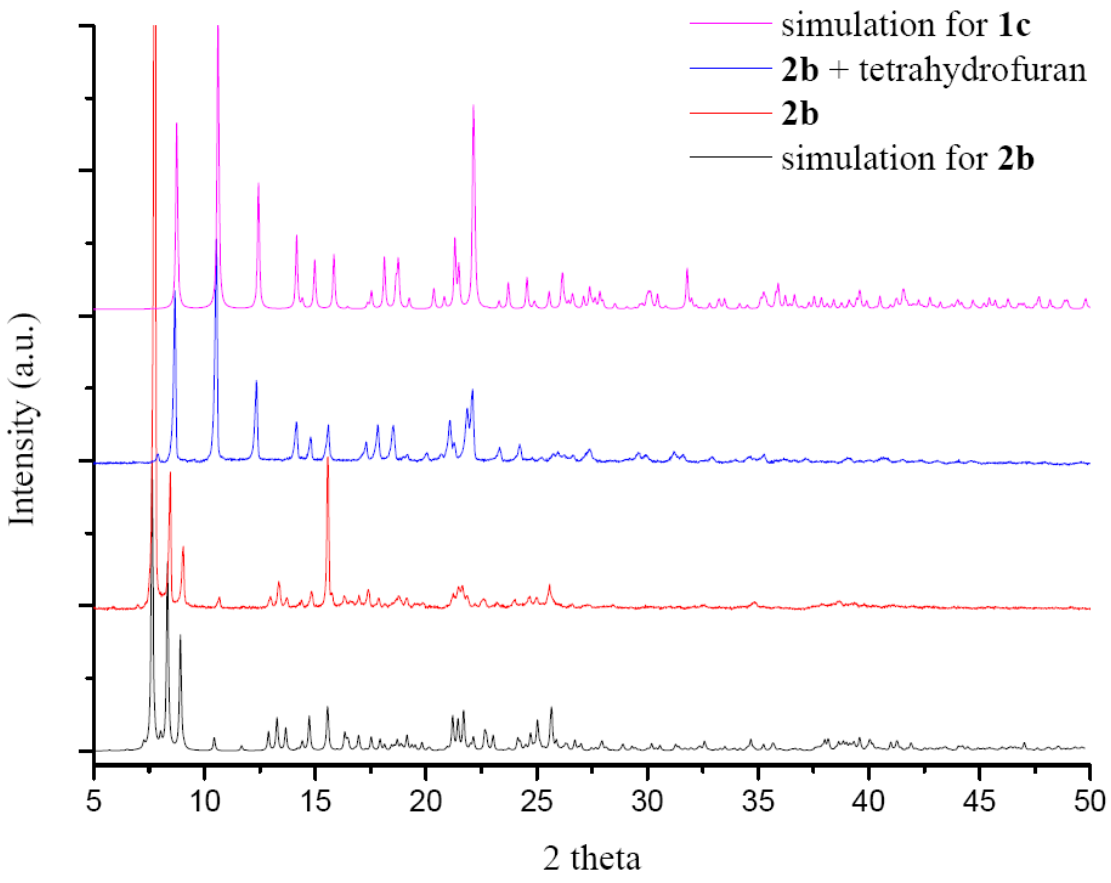

Fig. S21. The simulated and solvent-induced SCSC transformation PXRD patterns for **2b** to **1c**.

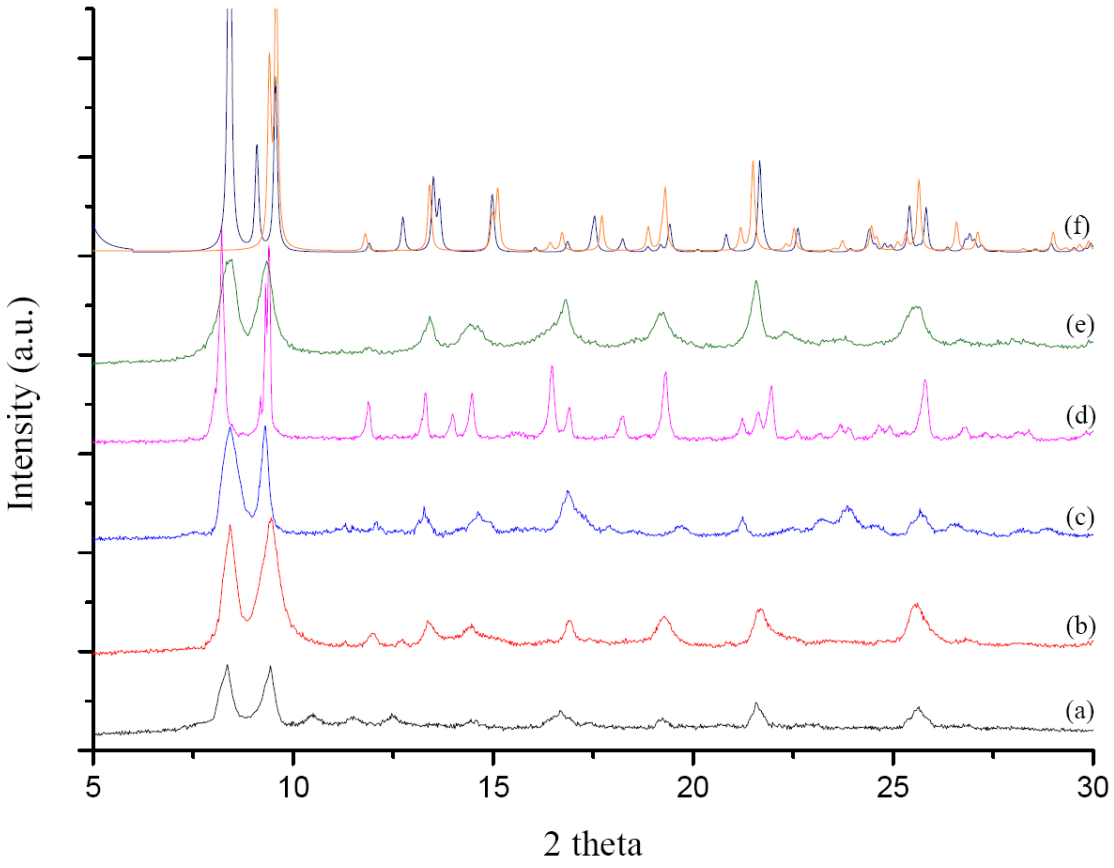

Fig. S22. The PXRD patterns for the desolvated complexes of (a) **1a**, (b) **1b**, (c) **1c**, (d) **2a**, (e) **2b**, (f) **2d** (deep blue line) and **2e** (orange line) at 240 ^{o}C.

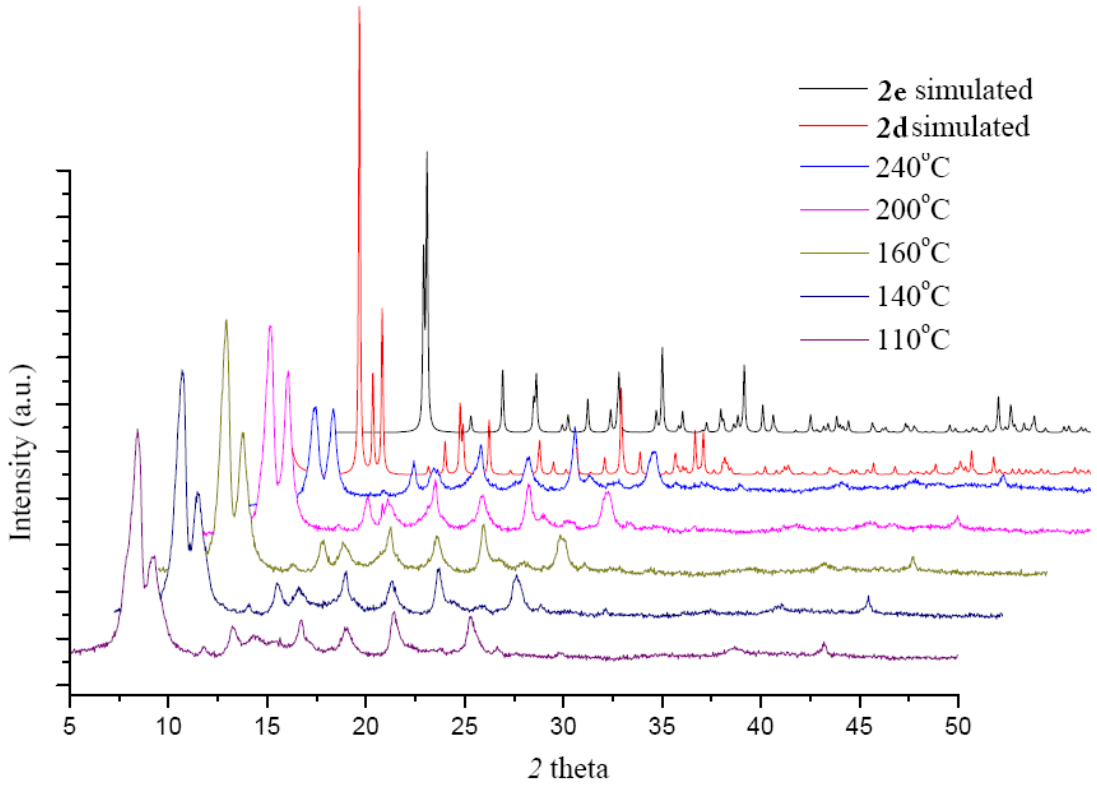

Fig. S23. The simulated and temperature-dependent PXRD patterns for **2b** at 110 °C to 240 °C

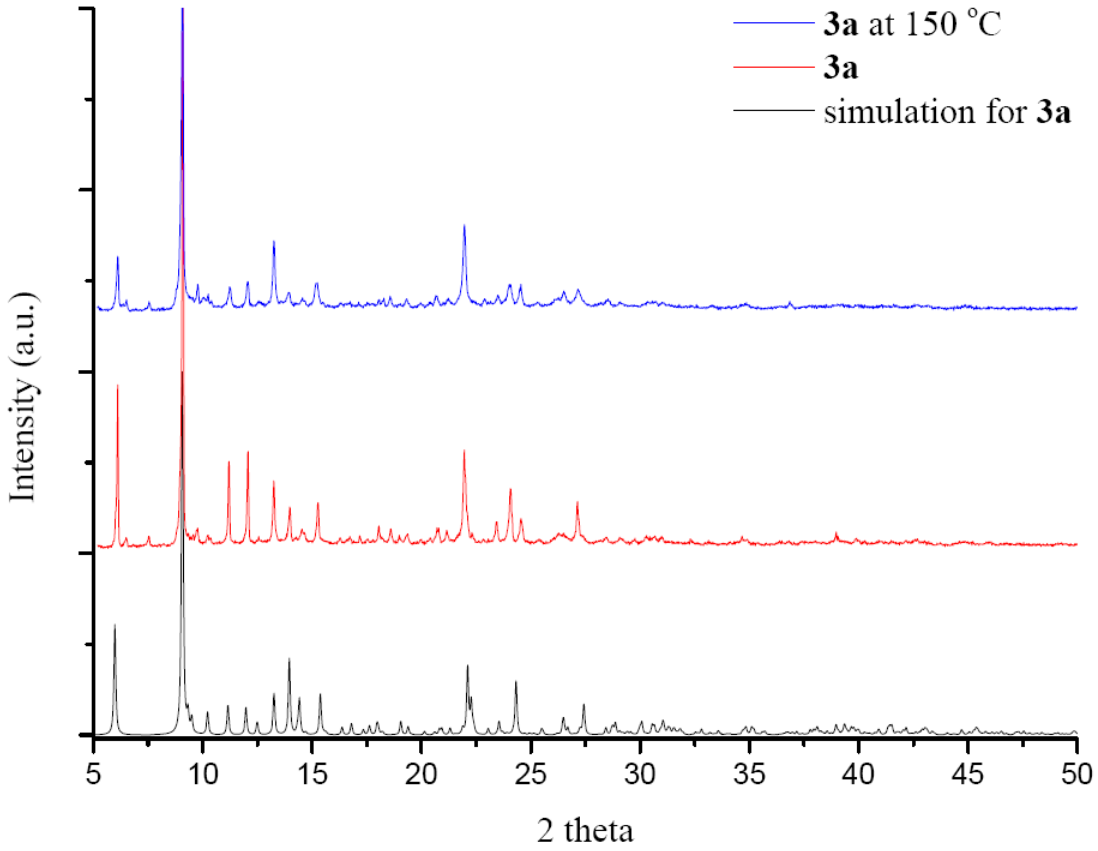

Fig. S24. Simulated, experimental and 150 °C powder XRD patterns for **3a**.

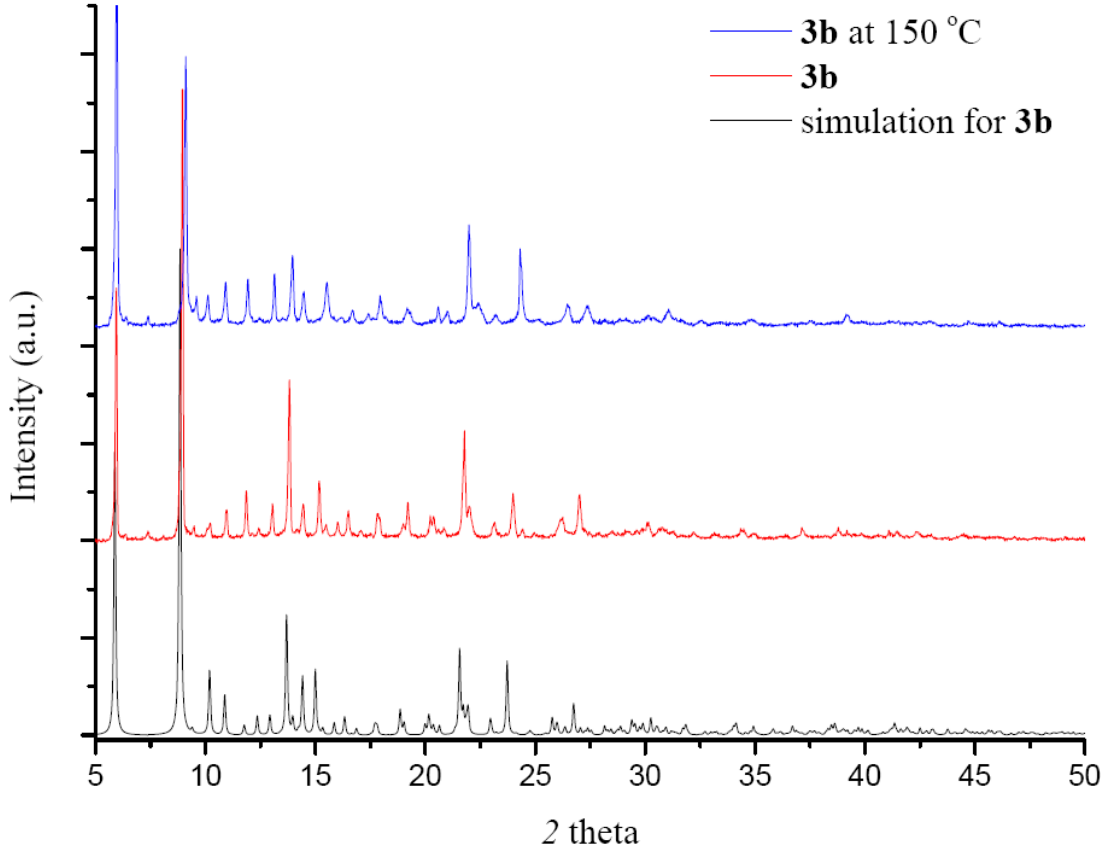

Fig. S25. Simulated, experimental and 150 °C powder XRD patterns **3b**.

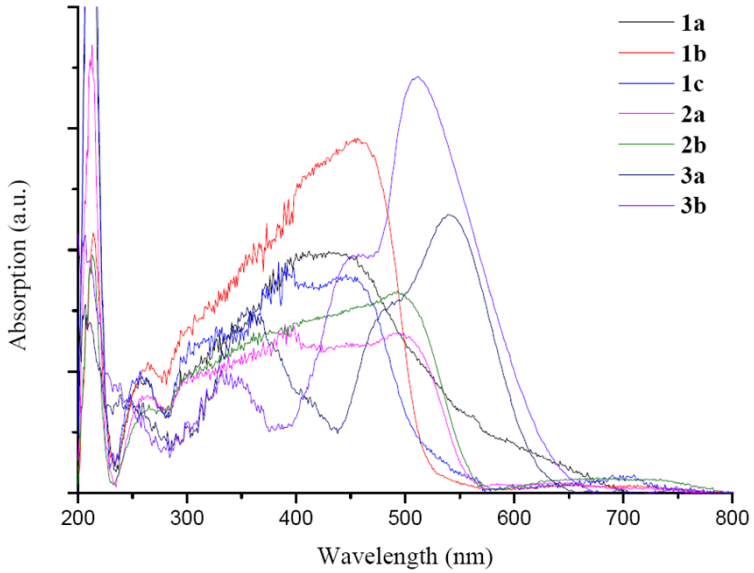

(a)

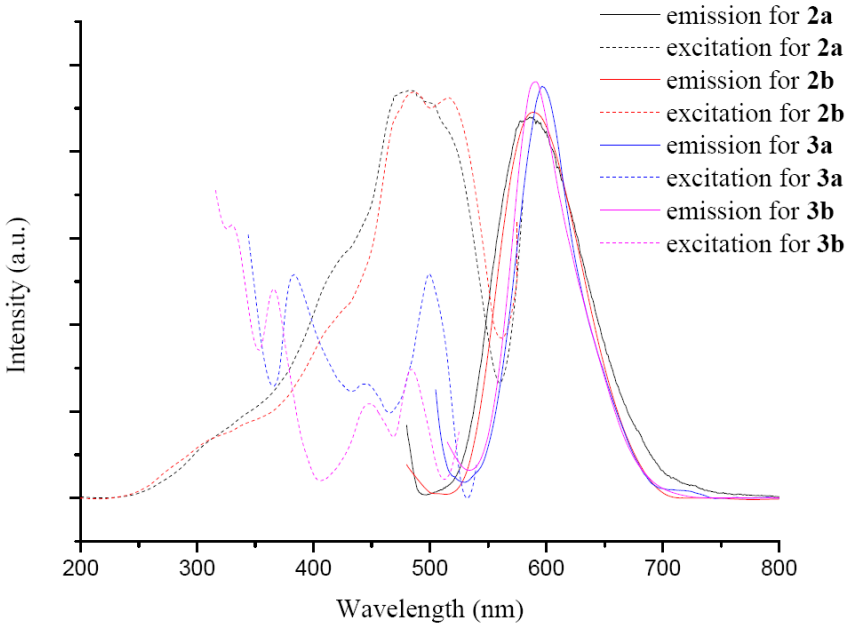

(b)

Fig. S26. (a) UV-vis spectra for absorption of complexes **1a** - **3b** in the solid state at room temperature. (b) emission and excitation spectra for crystalline complexes **2a** - **3b** (non-grounding).

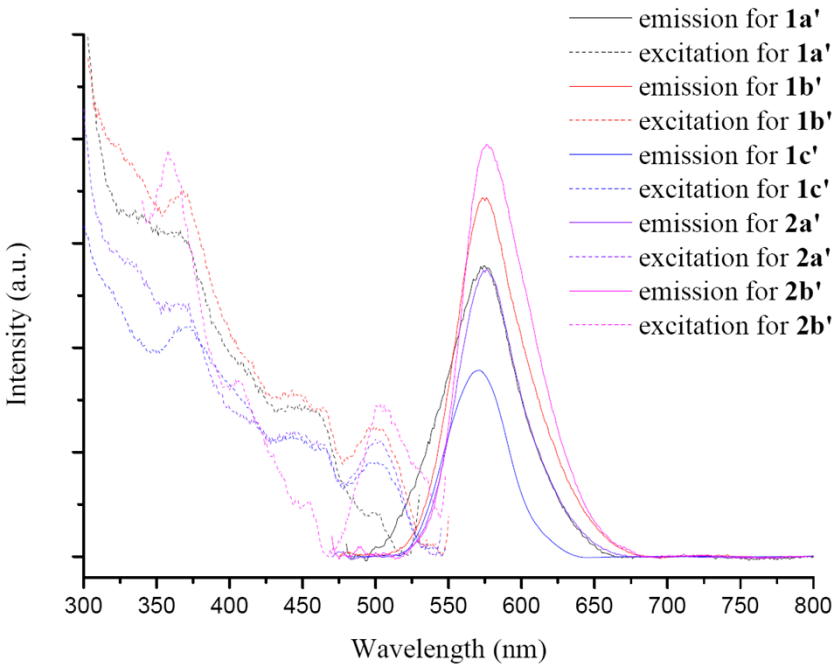

Fig. S27. The emission spectra of desolvated products of **1a** – **2b**.

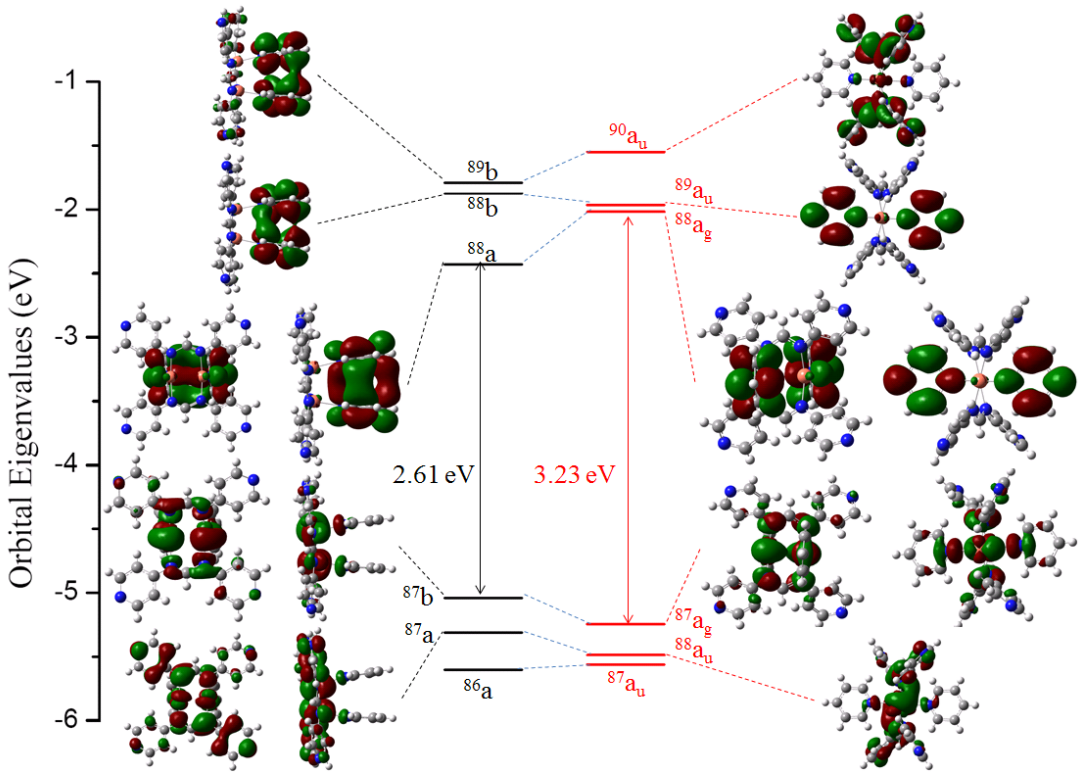

Fig. S28. The energy gap for *syn*- (left) and *anti*-geometrical (right) complexes as well as the electron contributions of HOMO-1, HOMO, LUMO, LUMO+1 and LUMO+2.

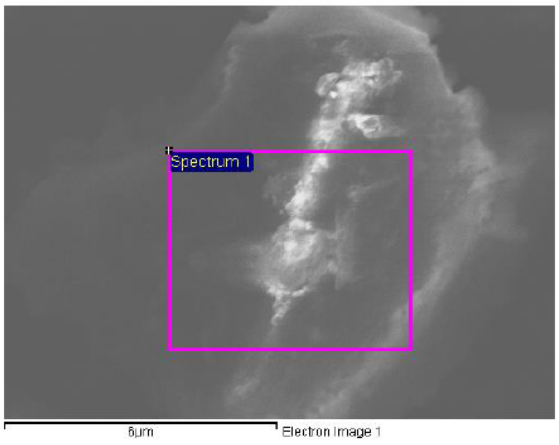

Element	Weight%	Atomic%
C K	41.56	61.85
N K	13.70	20.39
O K	5.87	6.56
Cl K	7.62	3.84
Cu L	19.52	5.49
Cd L	11.74	1.87
Totals	100.00	

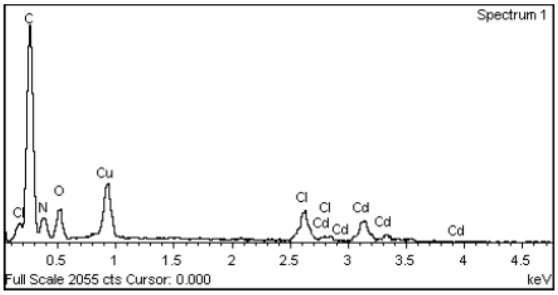

(a)

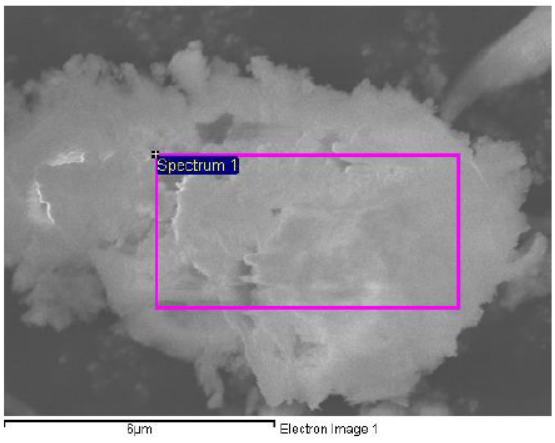

Element	Weight%	Atomic%
C K	46.66	66.20
N K	10.25	14.54
O K	9.36	9.96
Cl K	8.40	4.04
Cu L	12.08	3.24
Cd L	13.25	2.01
Totals	100.00	

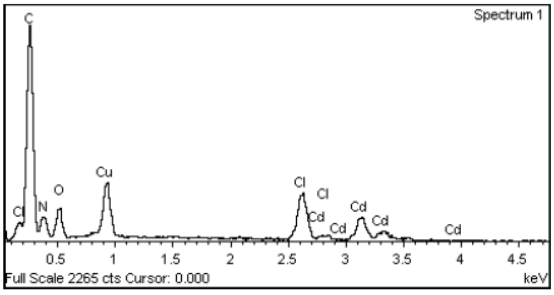

(b)

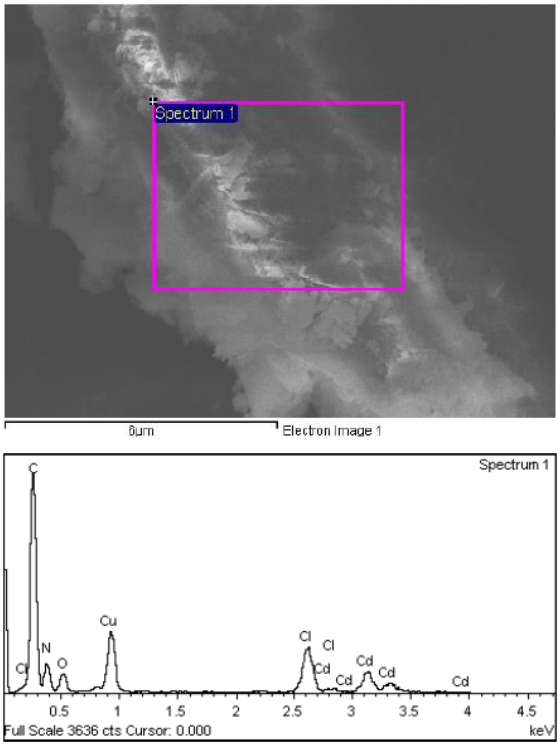

Element	Weight%	Atomic%
C K	38.46	57.01
N K	16.70	24.76
O K	6.54	7.27
Cl K	9.10	4.57
Cu L	14.42	4.04
Cd L	14.79	2.34
Totals	100.00	

(c)

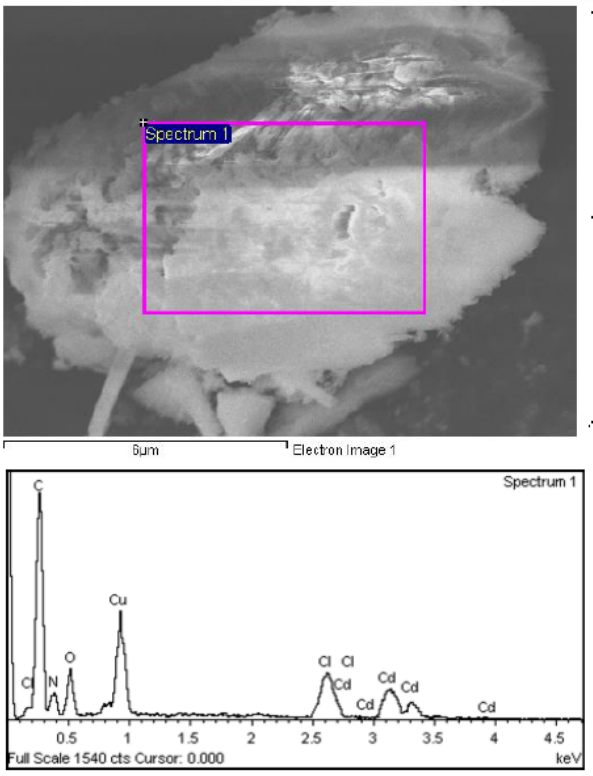

Element	Weight%	Atomic%
C K	32.10	56.64
N K	7.73	13.65
O K	9.30	12.32
Cl K	12.38	7.40
Cu L	18.83	6.28
Cd L	19.65	3.71
Totals	100.00	

(d)

Fig. S29. The SEM images and EDS spectra of the complexes obtained by adding (a) 0.50 mmol, (b) 1.00 mmol, (c) 1.50 mmol and (d) 2.00 mmol to 1 mmol of **1a** in 20 mL ACT.

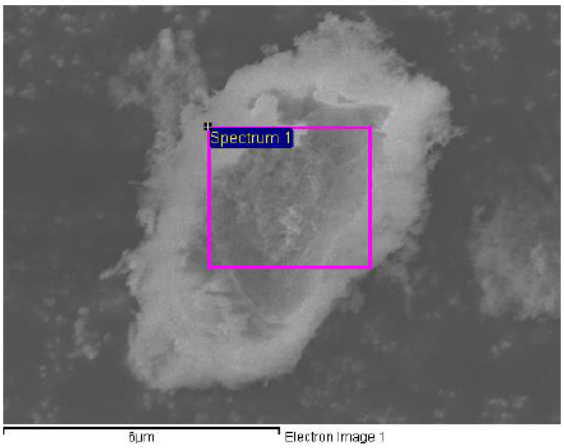

Element	Weight%	Atomic%
C K	41.86	63.02
N K	12.80	19.27
O K	5.37	6.07
Cl K	8.26	4.22
Cu L	18.77	5.34
Cd L	12.95	2.08
Totals	100.00	

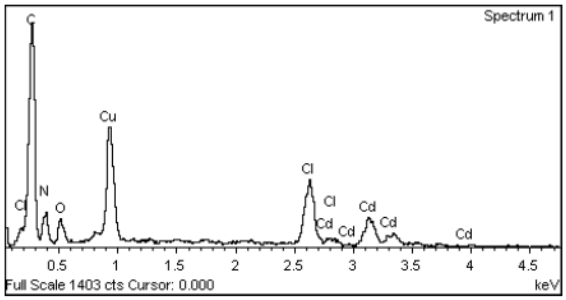

(a)

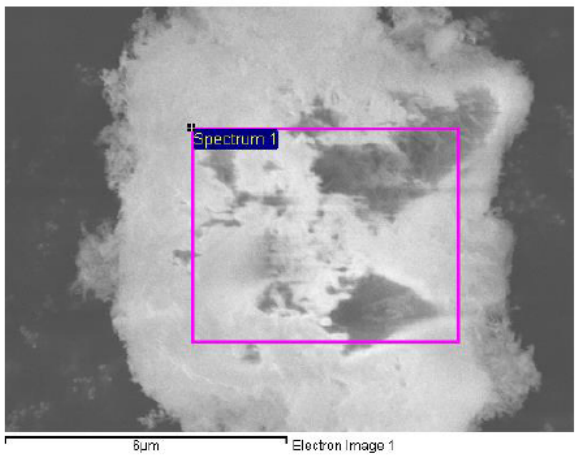

Element	Weight%	Atomic%
C K	40.68	62.16
N K	12.79	19.55
O K	5.29	6.07
Cl K	10.48	5.42
Cu L	14.20	4.10
Cd L	16.57	2.71
Totals	100.00	

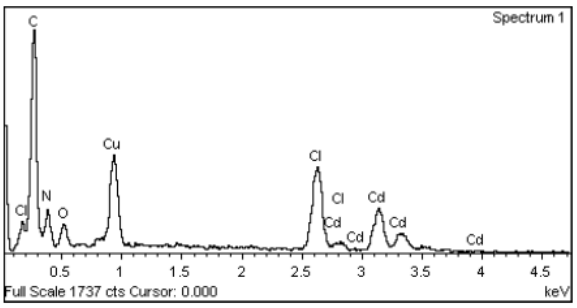

(b)

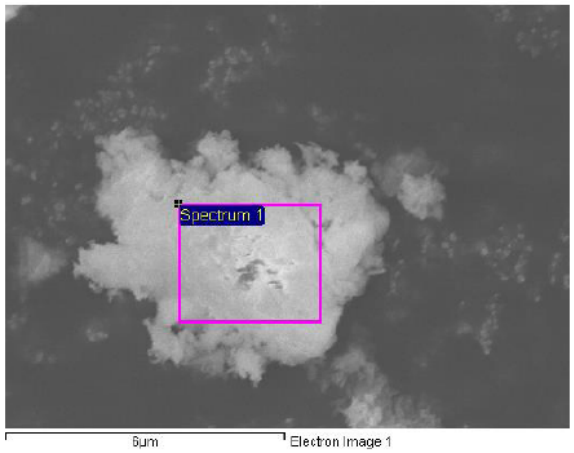

Element	Weight%	Atomic%
C K	48.83	68.61
N K	10.29	14.46
O K	7.27	7.67
Cl K	8.98	4.27
Cu L	11.18	2.97
Cd L	13.45	2.02
Totals	100.00	

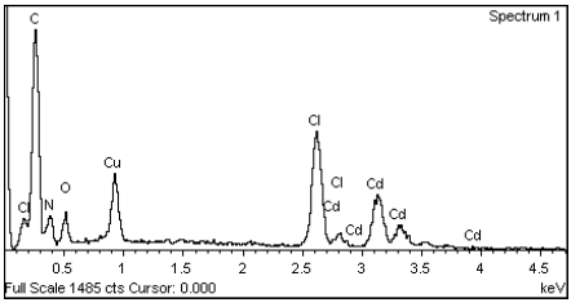

(c)

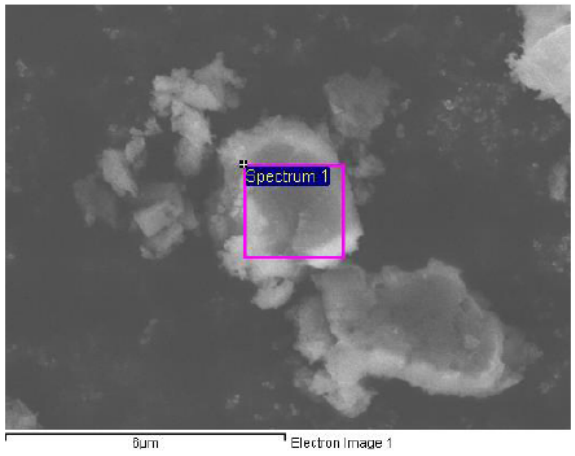

Element	Weight%	Atomic%
C K	33.54	57.41
N K	11.86	20.30
O K	4.31	5.54
Cl K	12.95	7.51
Cu L	17.09	5.53
Cd L	20.26	3.71
Totals	100.00	

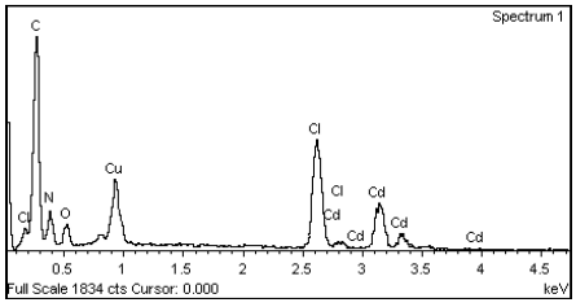

(d)

Fig. S30. The SEM images and EDS spectra of the complexes obtained by adding (a) 0.50 mmol, (b) 1.00 mmol, (c) 1.50 mmol and

(d) 2.00 mmol to 1 mmol of **2a** in 20 mL MeOH.

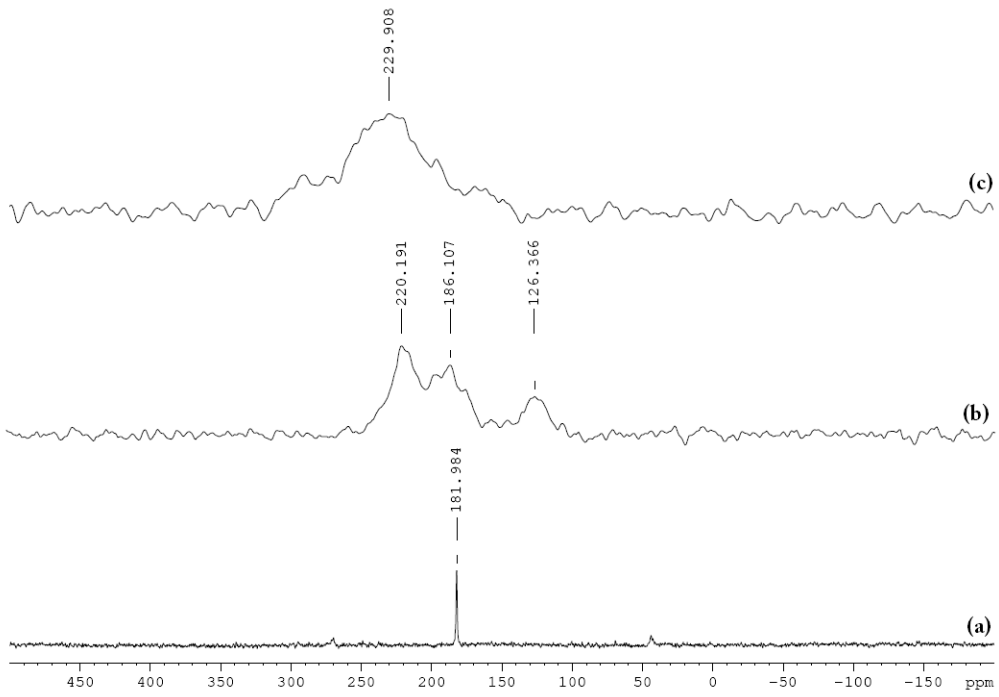

Fig. S31. The ^{113}Cd solid-state NMR spectra of (a) $CdCl_2$ metal salts, (b) $CdCl_2$ in **1a**, and (c) $CdCl_2$ in **2a**.

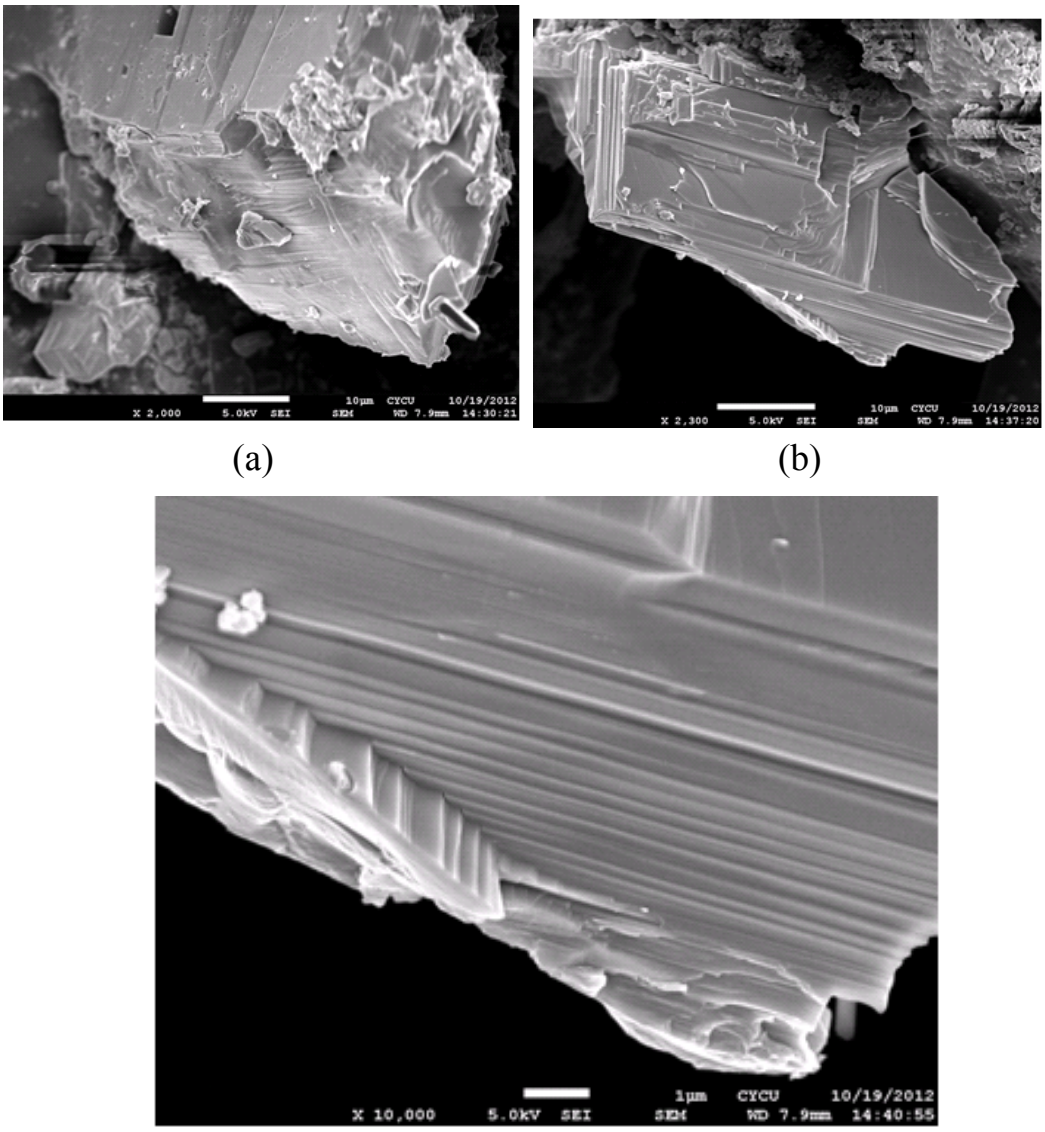

(a) (b)

(c)

Fig. S32. SEM images of **2b** at RT. Using an accelerating voltage of 5.0 kV and (a) a magnification of 2000x, scale bar is 10 μm, (b) a magnification of 2300x, scale bar is 10 μm, (c) a magnification of 10000x, scale bar is 1 μm.

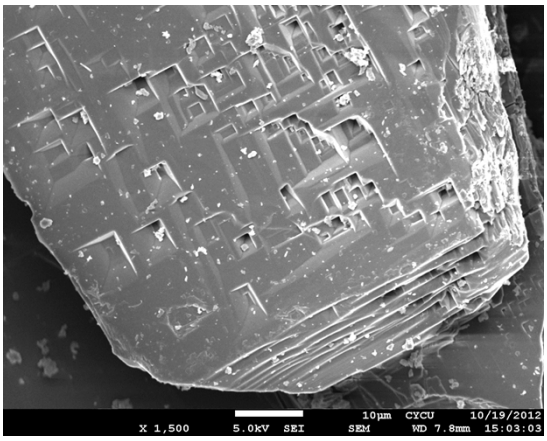

(a)

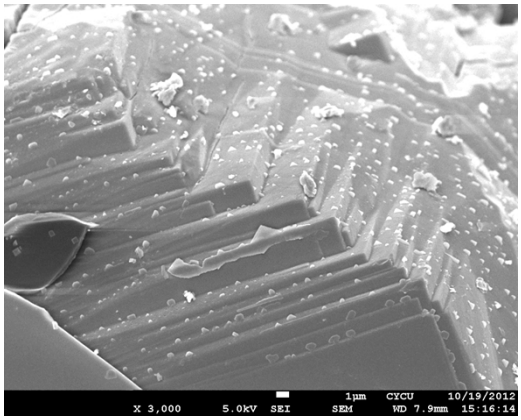

(b)

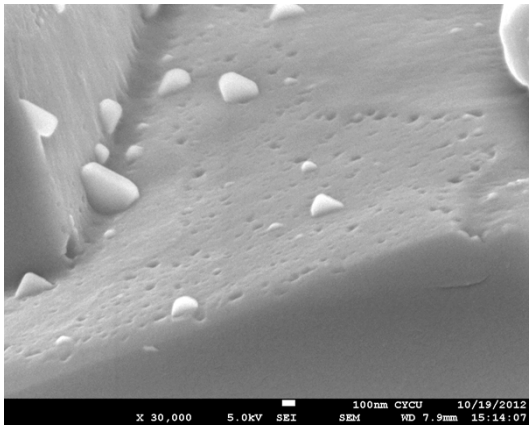

(c)

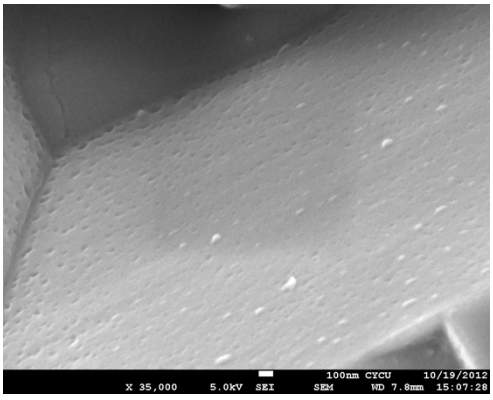

(d)

Fig. S33. Four SEM images showing the defects of **2b** after heated at 180 ^{o}C. Using an accelerating voltage of 5.0 kV and (a) a magnification of 1500x, scale bar is 10 μm, (b) a

magnification of 3000x, scale bar is 1 μm, (c) a magnification of 30000x, scale bar is 100 nm, (d) a magnification of 35000x, scale bar is 100 nm.